Supporting Information

Adaptive Chirality of Achiral Tetraphenylethene-Based Tetracationic Cyclophanes with Dual Responses of Fluorescence and Circular Dichroism in Water

Haiyang Zhang, Lin Cheng, Hao Nian, Jiang Du, Tao Chen, and Liping Cao*

College of Chemistry and Materials Science, Northwest University, Xi'an, 710069, P. R. China.

E-mail: chcaoliping@nwu.edu.cn

Table of Contents **Pages**

Experimental Procedures

General Experimental Details. Starting materials were purchased from commercial suppliers were used without further purification. Melting points were recorded by using a WRS-1A apparatus in open capillary tubes. IR spectra were measured on a TENSOR27 spectrometer. NMR spectra were recorded on a spectrometer operating at 400 MHz and 600 MHz for ^{1}H and 100 MHz and 150 MHz for ^{13}C NMR spectra on a Bruker ascend 400 spectrometer and JEOL 600 spectrometer. Mass spectrometry was performed using an Electron Spray Ionization (ESI) on a Ultimate3000 and a Micromass Quattro II triplequadrupole mass spectrometer using electrospray ionization with a MassLynx operating system. UV/vis spectra were done on Agilent Cary-100 spectrometer. Fluorescence spectra were performed by using a Horiba Fluorolog-3 spectrometer. SEM images were obtained on Hitachi SU8010 microscope. Isothermal titration calorimetry (ITC) was carried out using a VP-ITC (Malvern) at 25 ˚C, and computer fitting of the data were performed using the VP-ITC analyze software. The Circular dichroism (CD) spectra were recorded on a J-1500 spectropolarimeter, using a 1 cm quartz cuvette. DLS and Zeta-Potential was measured on a Brookhaven 90Plus PALS. Confocal laser scanning microscope images were obtained on Nikon $C2^{+}$ confocal microscope.

Synthetic Procedures and Characterization Data

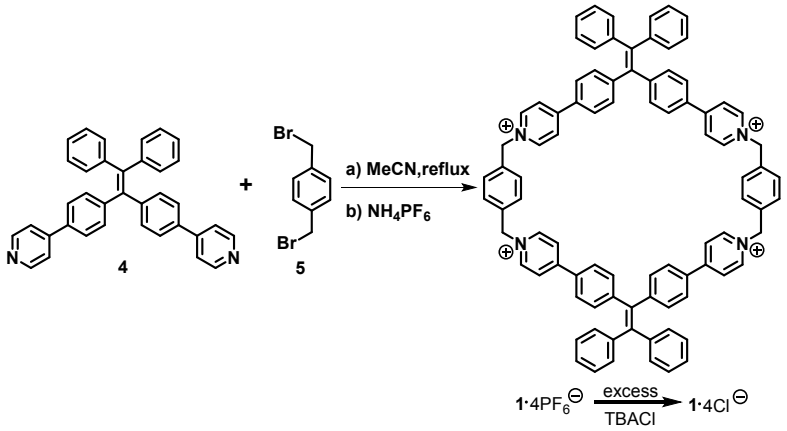

Compound 1•4PF$_6^-$. A 250 mL two-necked flask was charged with **4** (100 mg, 0.21 mmol), **5** (54 mg, 0.20 mmol), dry MeCN (100 mL) and the suspension was heated at

85 °C for 3 days. The reaction mixture was then cooled to ambient temperature and collected precipitate. The precipitate was washed with MeCN (3 × 20 mL) to give rise to a yellow solid. To exchange Br^- counterions to PF_6^- the solid was dissolved in H_2O (10 mL), adding excess amount of NH_4PF_6 (300 mg) and the mixture was stirred for 12 h. The precipitate was collected and washed with H_2O (3 × 20 mL) to give rise to a yellow solid (70 mg). The final powder product was purified by column chromatography, with $CHCl_3$: MeCN (saturated NH_4PF_6) = 4:1 (v:v) mobile phase (yield: 13.8%). M.p. > 300 °C. IR (KBr, cm^{-1}): 3441s, 1638s, 1601m, 1497m, 1163m, 1015m, 841s, 557m. ^{1}H NMR (600 MHz, CD_3CN): 8.61 (d, J = 7.0, 8H), 8.14 (d, J = 7.0, 8H), 7.69 (d, J = 8.4, 8H), 7.53 (s, 8H), 7.27 (d, J = 8.4, 8H), 7.25-7.15 (m, 12H), 7.15-7.05 (m, 8H), 5.68 (s, 8H). ^{13}C NMR (150 MHz, CD_3CN): 156.9, 148.6, 145.7, 145.2, 143.7, 139.2, 135.5, 133.3, 132.6, 131.8, 131.1, 129.0, 128.6, 128.3, 125.8, 63.8. ESI-TOF-MS: m/z 735.2295 ([**1**•4PF_6^- − 2PF_6^-]$^{2+}$, calcd. for $[C_{88}H_{68}N_4P_2F_{12}]^{2+}$, 735.2358); 441.8335 ([**1**•4PF_6^- − 3PF_6^-]$^{3+}$, calcd. for $[C_{88}H_{68}N_4PF_6]^{3+}$, 441.8356); 295.1326 ([**1**•4PF_6^- - 4PF_6^-]$^{4+}$, calcd. for $[C_{88}H_{68}N_4]^{4+}$, 295.1356).

Compound 1•4Cl$^-$. **1**•4PF_6^- (50 mg, 0.03 mmol) was dissolved in MeCN (5 mL), adding excess amount of tetrabutylammoium choride hydrate (TBACl, 10 mg) and the mixture was stirred for 12 h. The precipitate was collected and washed with MeCN (3×10 mL) to give rise to a yellow solid (yield: 83.3%). M.p. > 300 °C. IR (KBr, cm^{-1}): 3431s, 1638s, 1601s, 1497m, 1408m, 1165m, 800m, 704m. ^{1}H NMR (600 MHz, CD_3OD): 8.96 (d, J = 7.0, 8H), 8.32 (d, J = 7.0, 8H), 7.80 (d, J = 8.5, 8H), 7.68 (s, 8H), 7.28 (d, J = 8.5, 8H), 7.20-7.10 (m, 12H), 7.10-7.05 (m, 8H), 5.85 (s, 8H). ^{13}C NMR (150 MHz, CD_3OD): 157.4, 149.1, 146.6, 145.7, 144.0, 139.5, 136.4, 133.9, 133.2, 132.3, 131.6, 129.1, 128.9, 128.6, 125.9, 64.0. ESI-TOF-MS: m/z 626.2511 ([**1**•4Cl^--2Cl^-]$^{2+}$, calcd. for $[C_{88}H_{68}N_4Cl_2]^{2+}$, 626.2410); 405.1733 ([**1**•4Cl^- − 3Cl^-]$^{3+}$, calcd. for $[C_{88}H_{68}N_4Cl]^{3+}$, 405.1705); 295.1392 ([**1**•4Cl^- − 4Cl^-]$^{4+}$, calcd. for $[C_{88}H_{68}N_4]^{4+}$, 295.1356).

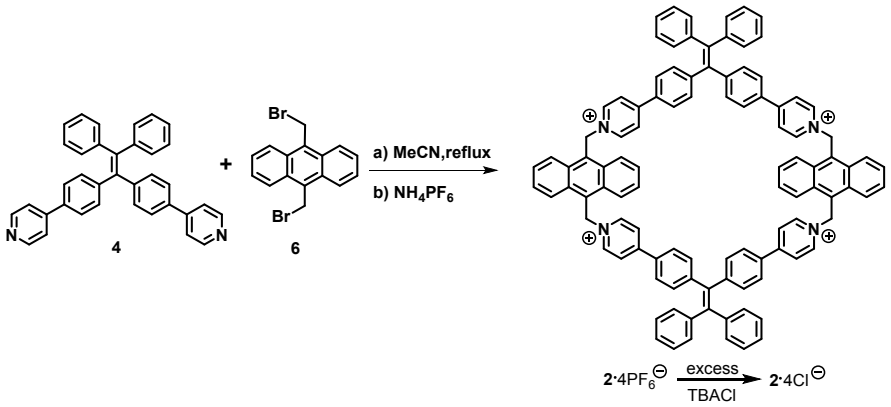

Compound 2•4PF$_6^-$. A 250 mL two-necked flask was charged with **4** (100 mg, 0.21 mmol), **6** (82 mg, 0.23mmol), dry MeCN (100 mL) and the suspension was heated at 85 °C for 3 days. The reaction mixture was then cooled to ambient temperature and collected precipitate. The precipitate was washed with MeCN (3 × 20 mL) to give rise to a yellow solid. To exchange Br^- counterions to PF_6^- the solid was dissolved in H_2O (10 mL), adding excess amount of NH_4PF_6 (300 mg) and the mixture was stirred for 12 h. The precipitate was collected and washed with H_2O (3 × 20 mL) to give rise to a yellow solid (24 mg). The final powder product was purified by column chromatography, with $CHCl_3$: MeCN (saturated NH_4PF_6) = 4:1 (v:v) mobile phase (yield: 11.9%). M.p. > 300 °C. IR (KBr, cm^{-1}): 3441s, 1638s, 1601m, 1497m, 1151m, 841s, 702m, 557s. ^{1}H NMR (400 MHz, CD_3CN): 8.56 (d, J = 6.9, 8H), 8.36 (dd, J = 6.9 and 3.1, 8H), 8.03 (d, J = 6.9, 8H), 7.75 (dd, J = 6.9 and 3.1, 8H), 7.60 (d, J = 8.4, 8H), 7.30-7.15 (m, 20H), 7.15-7.05 (m, 8H), 6.77 (s, 8H). ^{13}C NMR (100 MHz, CD_3CN): 157.2, 148.3, 145.8, 144.5, 143.8, 139.1, 133.4, 132.9, 132.6, 131.9, 129.5, 129.0, 128.6, 128.4, 126.6, 126.1, 125.1, 56.7. ESI-TOF-MS: m/z 835.7529 ([**2**•4PF$_6^-$ − 2PF$_6^-$]$^{2+}$, calcd. for [$C_{104}H_{76}N_4P_2F_{12}$]$^{2+}$, 835.7688); 508.8463 ([**2**•4PF$_6^-$ − 3PF$_6^-$]$^{3+}$, calcd. for [$C_{104}H_{76}N_4PF_6$]$^{3+}$, 508.8576); 345.4019 ([**2**•4PF$_6^-$ − 4PF$_6^-$]$^{4+}$, calcd. for [$C_{104}H_{76}N_4$]$^{4+}$, 345.4020).

Compound 2•4Cl$^-$. **2**•4PF$_6^-$ (100 mg, 0.05 mmol) was dissolved in MeCN (5 mL), adding excess amount of tetrabutylammoium choride hydrate (TBACl, 15 mg) and the mixture was stirred for 12 h. The precipitate was collected and washed with MeCN (3×10 mL) to give rise to a yellow solid (yield: 85.2%). M.p. > 300 °C. IR (KBr, cm^{-1}): 3433s, 1636s, 1601m, 1495m, 1410m, 1151m, 772w, 704m. ^{1}H NMR (600 MHz,

CD_3OD): 8.84 (d, J = 6.9, 8H), 8.53 (dd, J = 6.9 and 3.0, 8H), 8.21 (d, J = 6.9, 8H), 7.77 (dd, J = 6.9 and 3.0, 8H), 7.71 (d, J = 8.5, 8H), 7.23 (d, J = 8.5, 8H), 7.20-7.15 (m, 12H), 7.10-7.05 (m, 8H), 7.01 (s, 8H). ^{13}C NMR (150 MHz, CD_3OD): 157.7, 148.8, 146.6, 145.2, 144.1, 139.5, 133.9, 133.5, 133.0, 132.3, 129.8, 129.1, 128.9, 128.6, 127.3, 126.1, 125.3, 56.6. ESI-TOF-MS: m/z 726.2840 ([**2**•4Cl^- − 2Cl^-]$^{2+}$, calcd. for [$C_{104}H_{76}N_4Cl_2$]$^{2+}$, 726.2727); 472.1941 ([**2**•4Cl^- − 3Cl^-]$^{3+}$, calcd. for [$C_{104}H_{76}N_4Cl$]$^{3+}$, 472.1925).

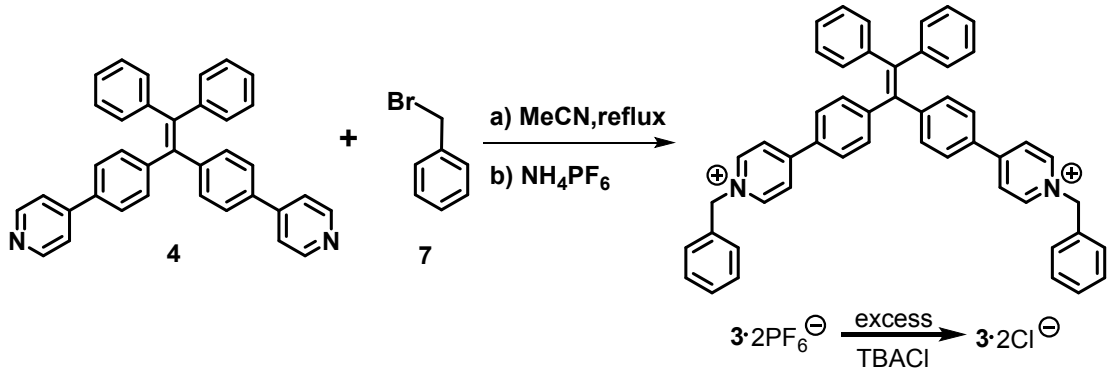

Compound 3•2PF_6^-. A 250 mL two-necked flask was charged with **4** (100 mg, 0.21 mmol), **7** (703 mg, 4.11mmol), dry MeCN (100 mL) and the suspension was heated at 85 °C for 3 days. The reaction mixture was then cooled to ambient temperature and collected precipitate. The precipitate was washed with MeCN (3 × 20 mL) to give rise to a yellow solid. To exchange Br^- counterions to PF_6^- the solid was dissolved in H_2O (10 mL), adding excess amount of NH_4PF_6 (300 mg) and the mixture was stirred for 12 h. The precipitate was collected and washed with H_2O (3 × 20 mL) to give rise to a yellow solid (153 mg) (yield: 77.7%). M.p. > 300 °C. IR (KBr, cm^{-1}): 1638s, 1601m, 1497m, 1161m, 837s, 700m, 557s. ^{1}H NMR (600 MHz, CD_3CN): 8.67 (d, J = 6.6, 4H), 8.17 (d, J = 6.6, 4H), 7.72 (d, J = 8.2, 4H), 7.55-7.40 (m, 10H), 7.30 (d, J = 8.2, 4H), 7.25-7.15 (m, 6H), 7.15-7.05 (m, 4H), 5.66 (s, 4H). ^{13}C NMR (150 MHz, CD_3CN): 156.7, 148.5, 145.6, 145.2, 143.6, 139.2, 134.1, 133.3, 132.6, 131.7, 130.7, 130.4, 129.9, 128.9, 128.6, 128.3, 125.8, 64.5. ESI-TOF-MS: m/z 813.3077 ([**3**•2PF_6^- − PF_6^-]$^+$, calcd. for [$C_{50}H_{40}N_2PF_6$]$^+$, 813.2828); 334.1663 ([**3**•2PF_6^- − 2PF_6^-]$^{2+}$, calcd. for [$C_{50}H_{40}N_2$]$^{2+}$, 334.1590).

Compound 3•2Cl$^-$. **3**•2PF_6^- (100 mg, 0.10 mmol) was dissolved in MeCN (5 mL), adding excess amount of tetrabutylammoium choride hydrate (TBACl, 15 mg) and the mixture was stirred for 12 h. The precipitate was collected and washed with MeCN (3×10 mL) to give rise to a yellow solid (yield: 86.4%). M.p. > 300 °C. IR (KBr, cm^{-1}): 1636s, 1599m, 1495m, 1161m, 814s, 700m, 617s. ^{1}H NMR (600MHz, CD_3OD): 8.98 (d, *J* = 6.3, 4H), 8.35 (d, *J* = 6.3, 4H), 7.83 (d, *J* = 8.0, 4H), 7.60-7.40 (m, 10H), 7.30 (d, *J* = 8.0, 4H), 7.20-7.05 (m, 10H), 5.82 (s, 4H). ^{13}C NMR (150 MHz, CD_3OD): 157.3, 149.0, 146.4, 145.7, 144.0, 139.6, 134.8, 133.9, 133.2, 132.2, 130.9, 130.7, 130.1, 129.1, 128.9, 128.5, 125.9, 64.7. ESI-TOF-MS: m/z 813.3077 ([**3**•2Cl$^-$ − Cl$^-$]$^+$, calcd. for $[C_{50}H_{40}N_2Cl]^+$, 813.2828); 334.1663 ([**3**•2Cl$^-$ − 2Cl$^-$]$^{2+}$, calcd. for $[C_{50}H_{40}N_2]^{2+}$, 334.1590).

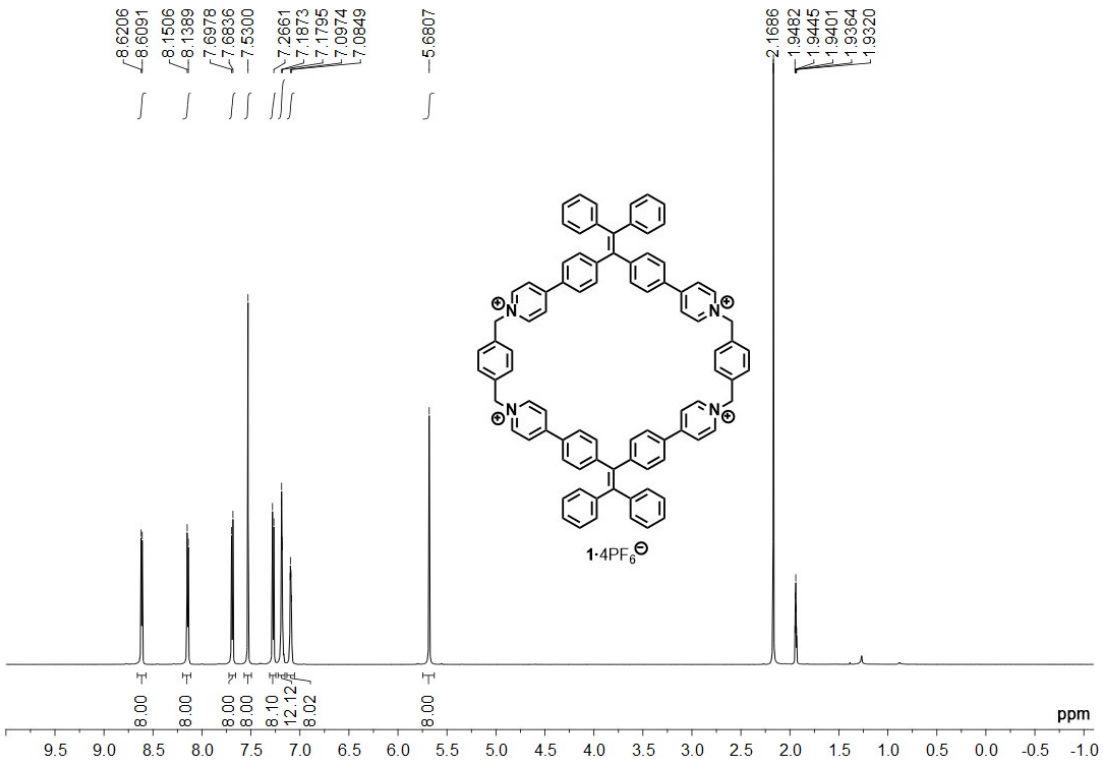

Figure S1. ^{1}H NMR spectrum recorded (600 MHz, CD_3CN, RT) for **1**•$4PF_6^-$.

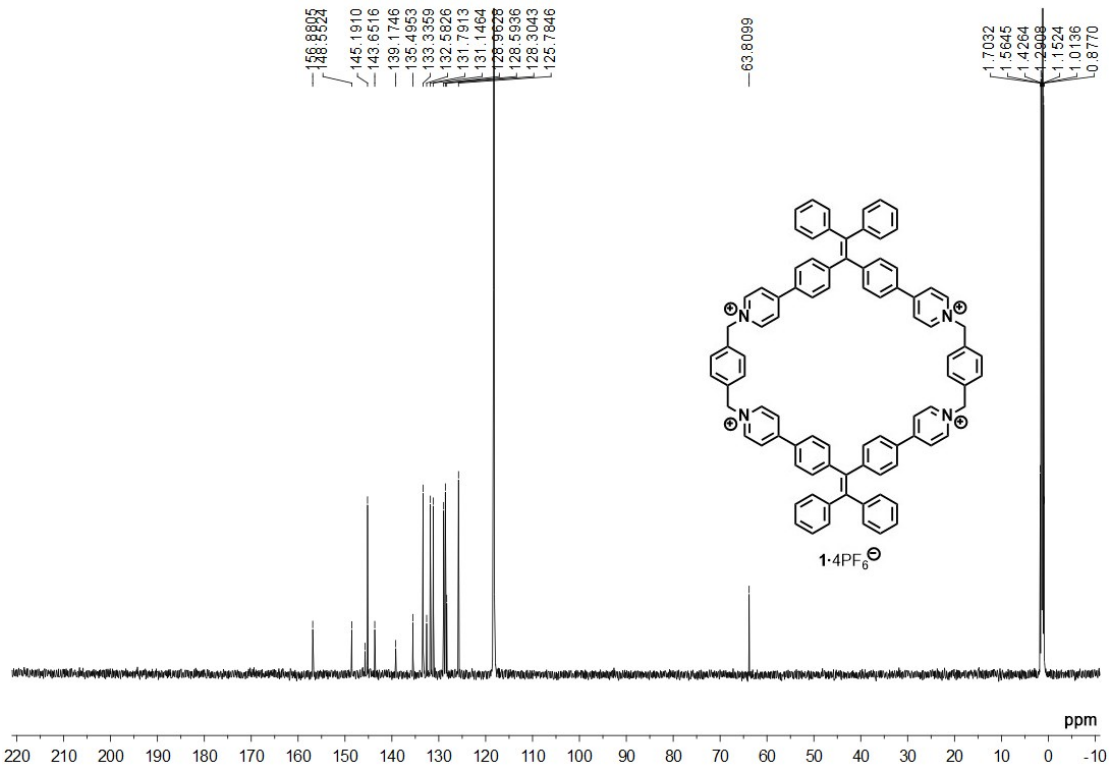

Figure S2. ^{13}C NMR spectrum recorded (150 MHz, CD_3CN, RT) for **1**•$4PF_6^-$.

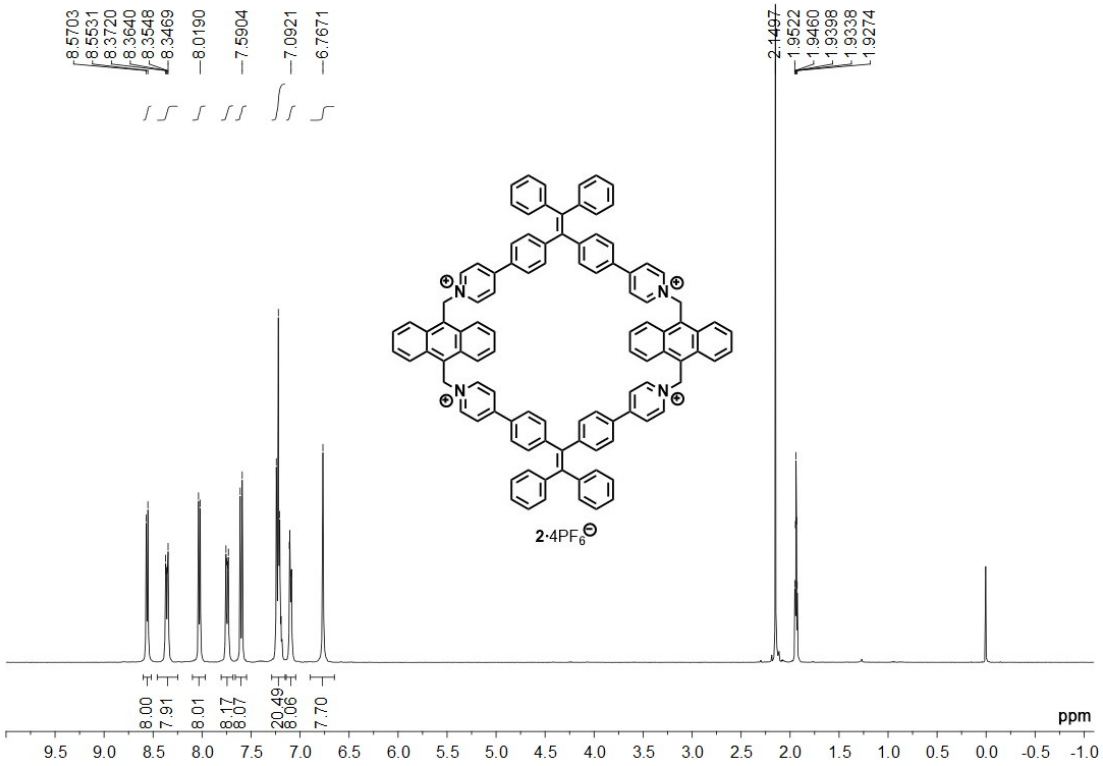

Figure S3. ^{1}H NMR spectrum recorded (400 MHz, CD_3CN, RT) for **2**•$4PF_6^-$.

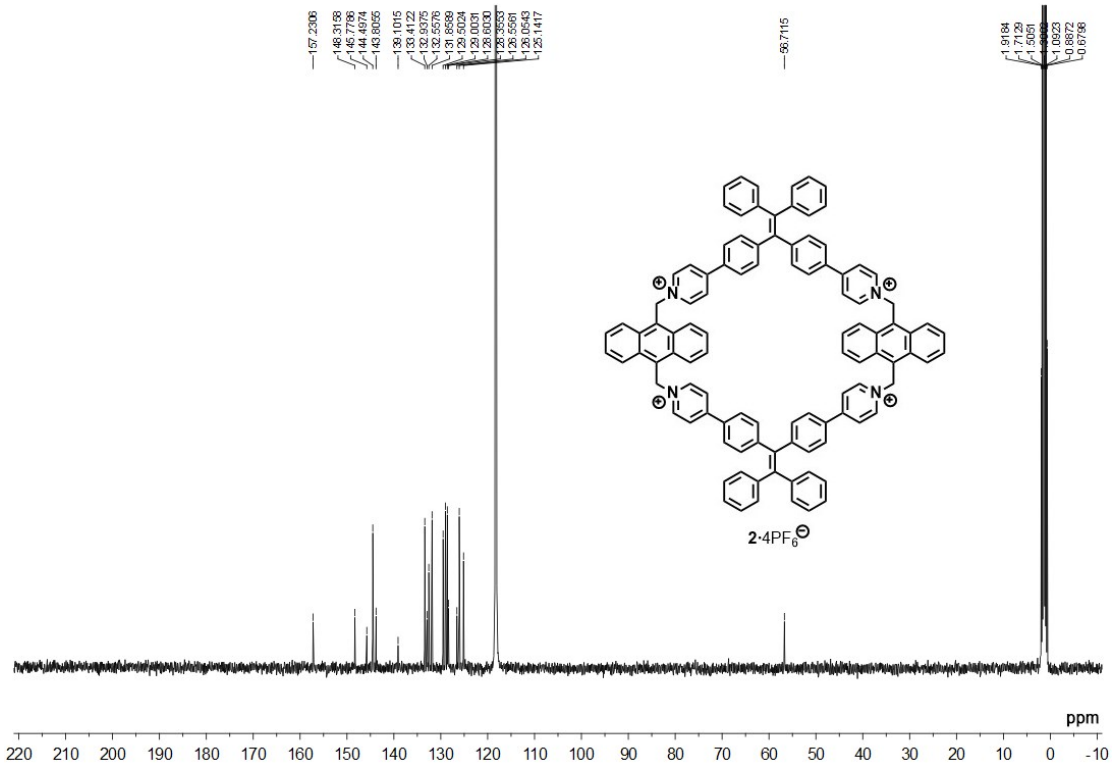

Figure S4. ^{13}C NMR spectrum recorded (100 MHz, CD_3CN, RT) for **2**•$4PF_6^-$.

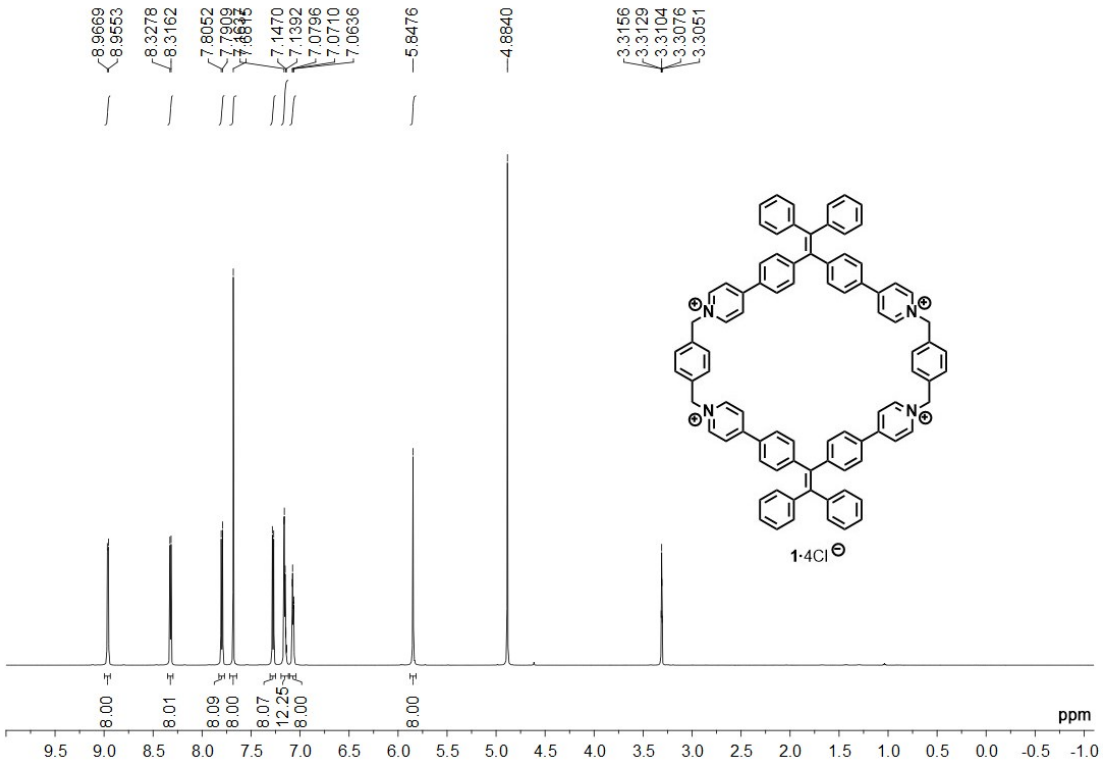

Figure S5. ^{1}H NMR spectrum recorded (600 MHz, CD_3OD, RT) for **1**•4Cl^{-}.

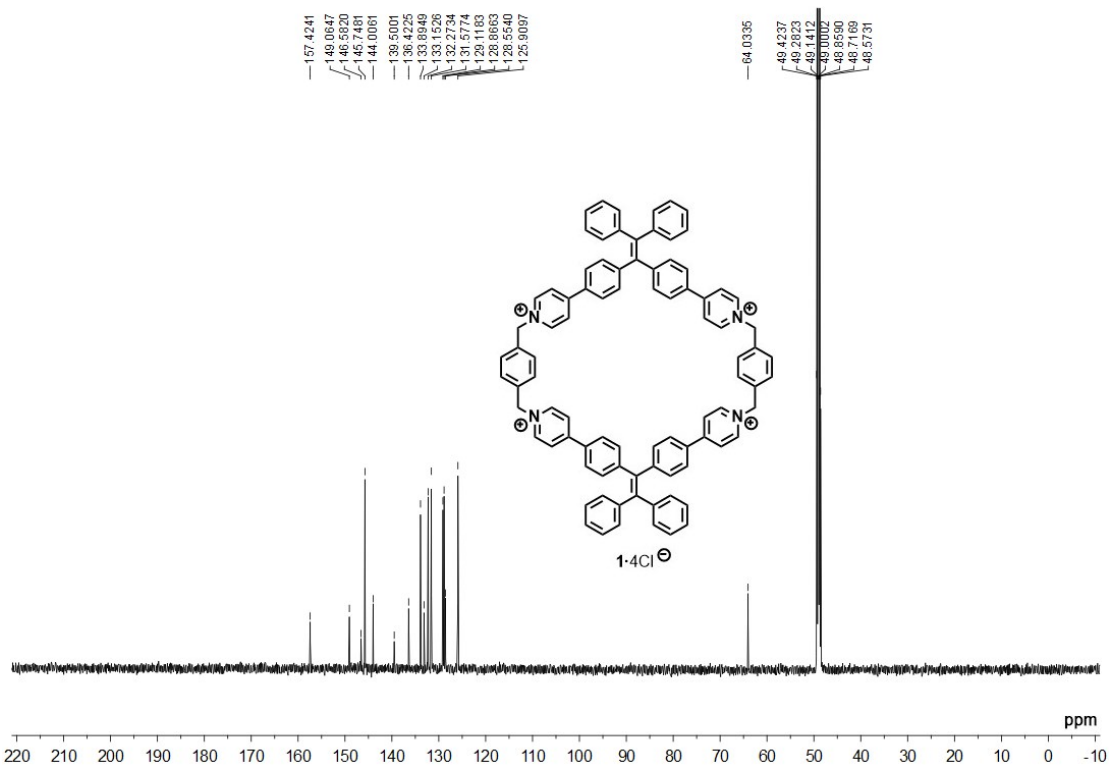

Figure S6. ^{13}C NMR spectrum recorded (150 MHz, CD_3OD, RT) for **1**•4Cl^{-}.

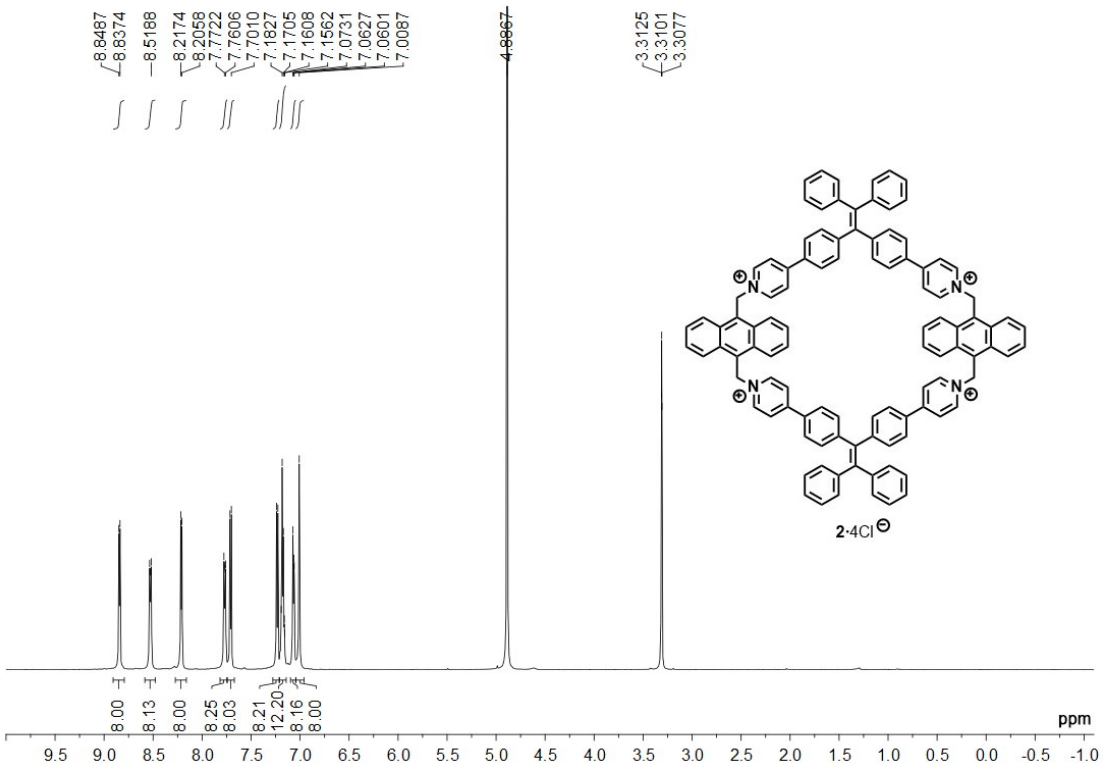

Figure S7. ^{1}H NMR spectrum recorded (600 MHz, CD_3OD, RT) for **2**•4Cl^{-}.

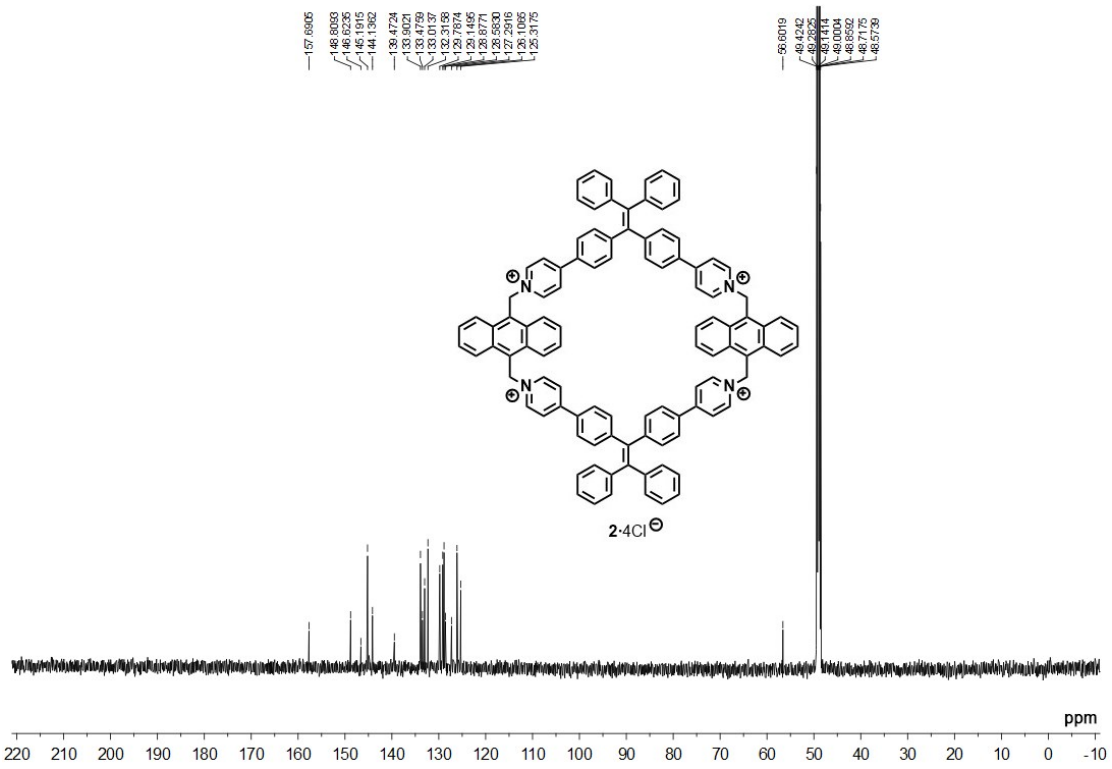

Figure S8. ^{13}C NMR spectrum recorded (150 MHz, CD_3OD, RT) for **2**•4Cl^{-}.

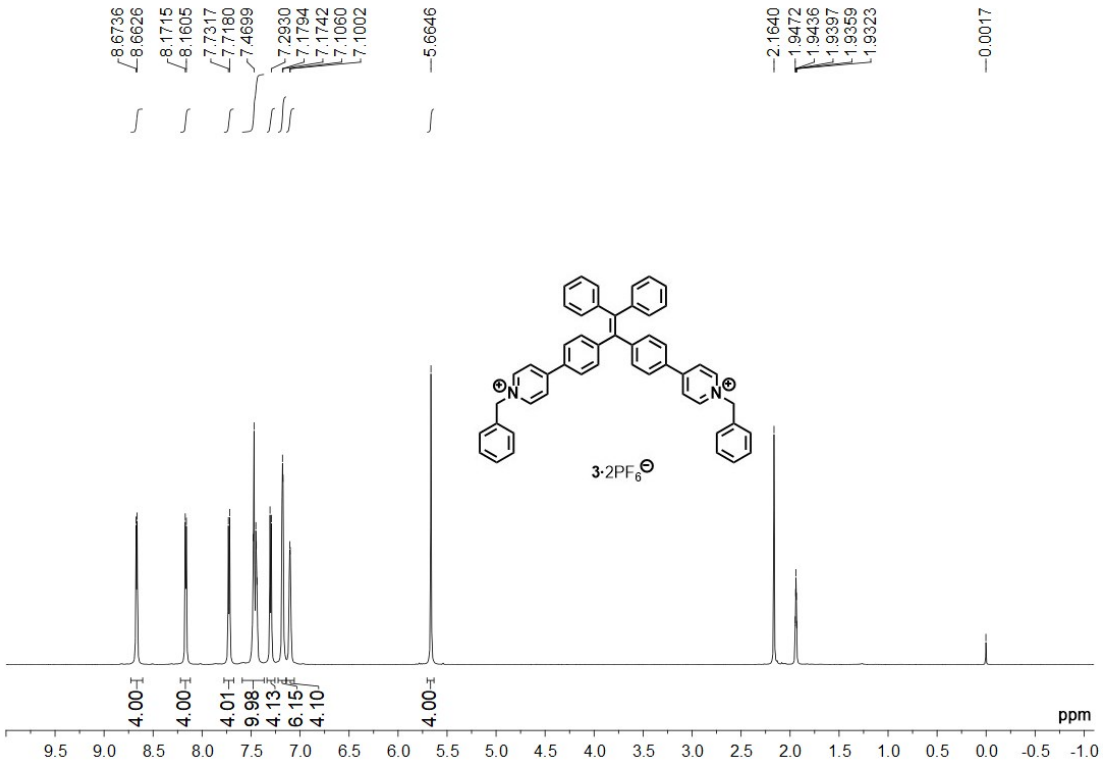

Figure S9. ^{1}H NMR spectrum recorded (600 MHz, CD_3CN, RT) for **3**•$2PF_6^-$.

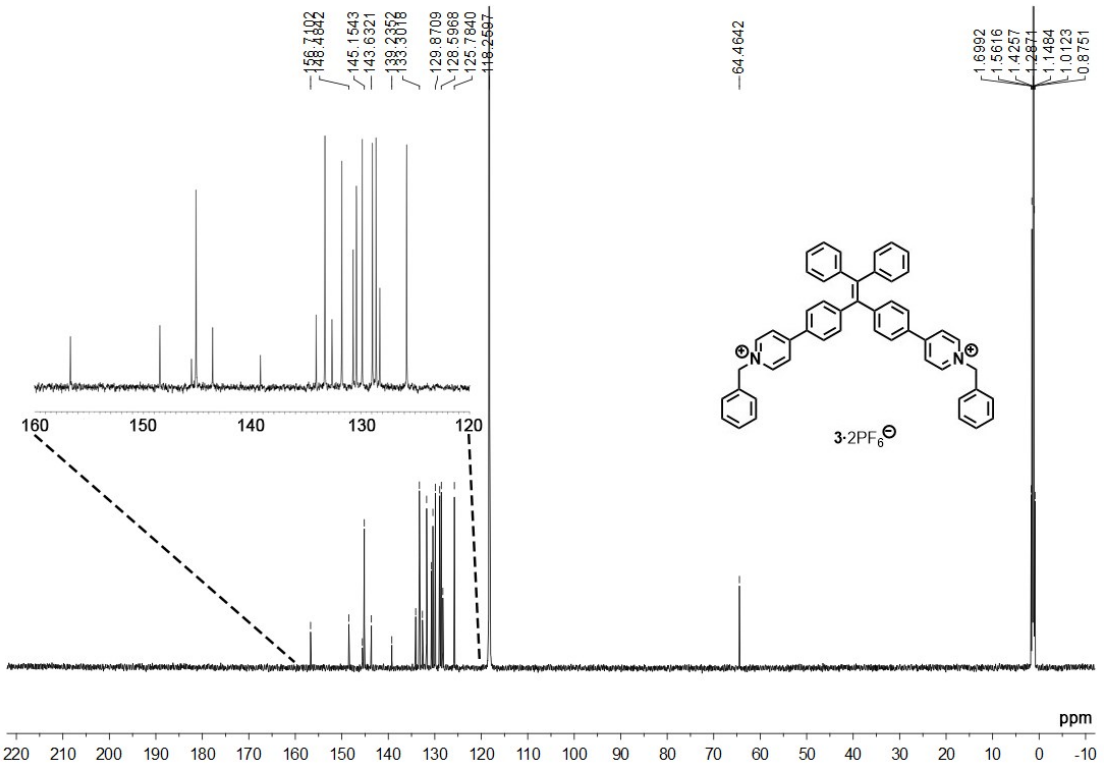

Figure S10. ^{13}C NMR spectrum recorded (150 MHz, CD_3OD, RT) for **3**•$2PF_6^-$.

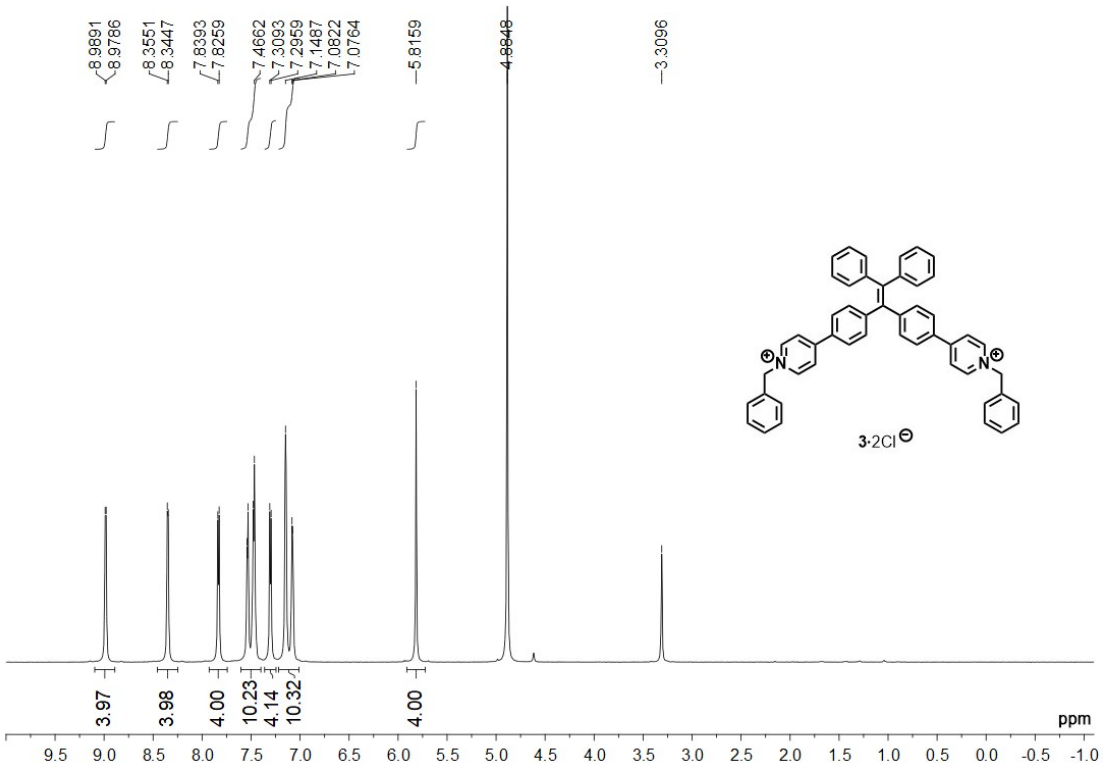

Figure S11. ^{1}H NMR spectrum recorded (600 MHz, CD_3CN, RT) for **3**•2Cl¯.

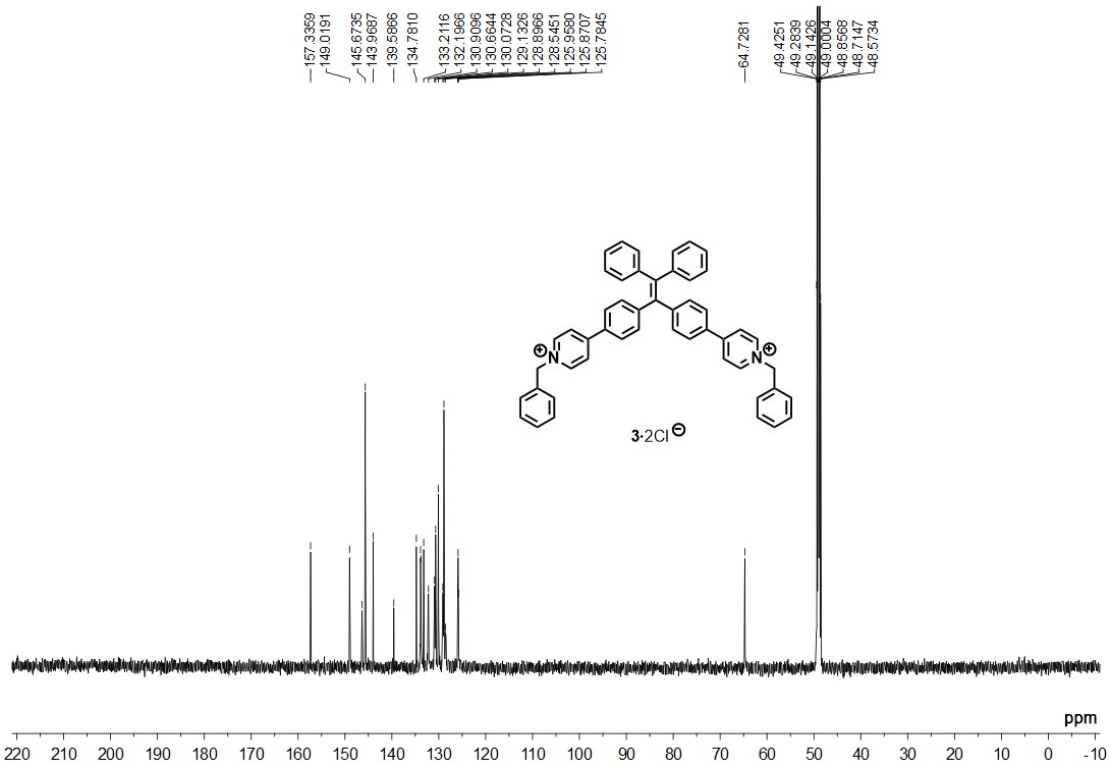

Figure S12. ^{13}C NMR spectrum recorded (150 MHz, CD_3OD, RT) for **3**•2Cl¯.

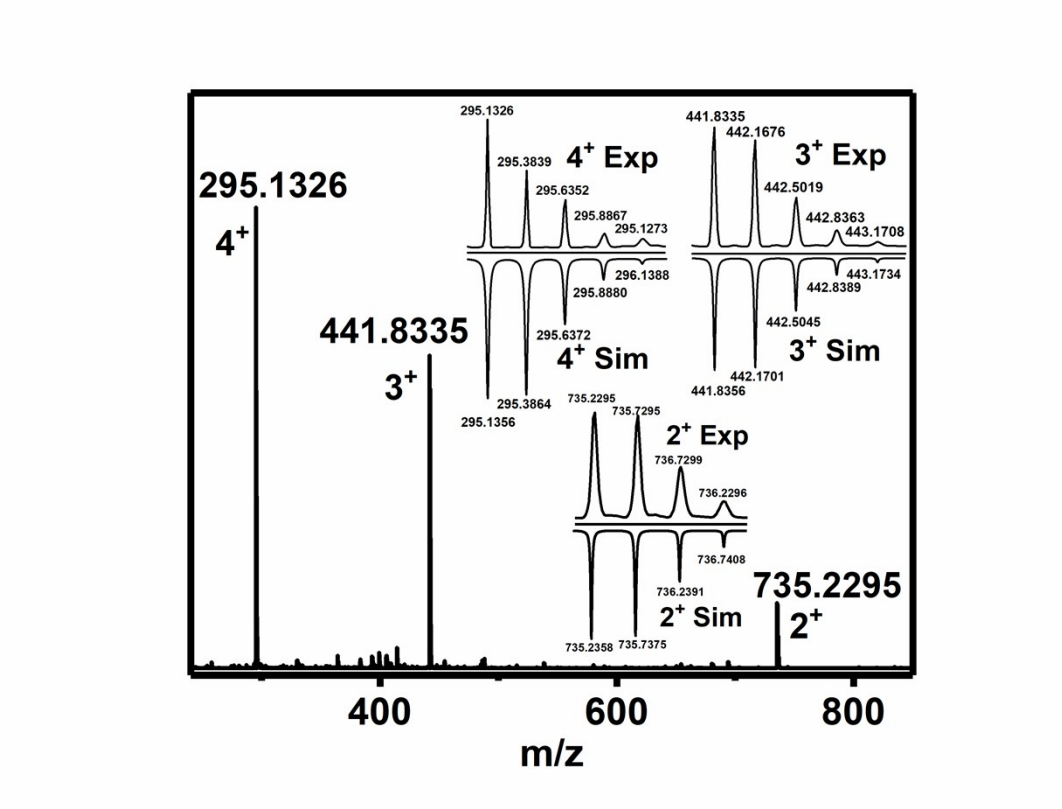

Figure S13. Experimental and calculated electrospray ionization mass spectra of **1**•4PF_6^-.

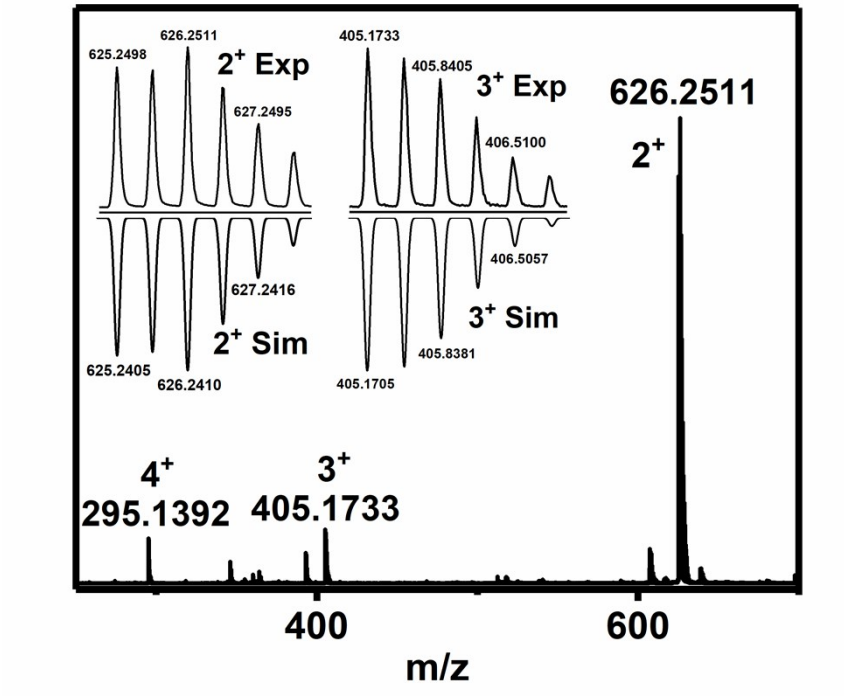

Figure S14. Experimental and calculated electrospray ionization mass spectra of **1**•4Cl^-.

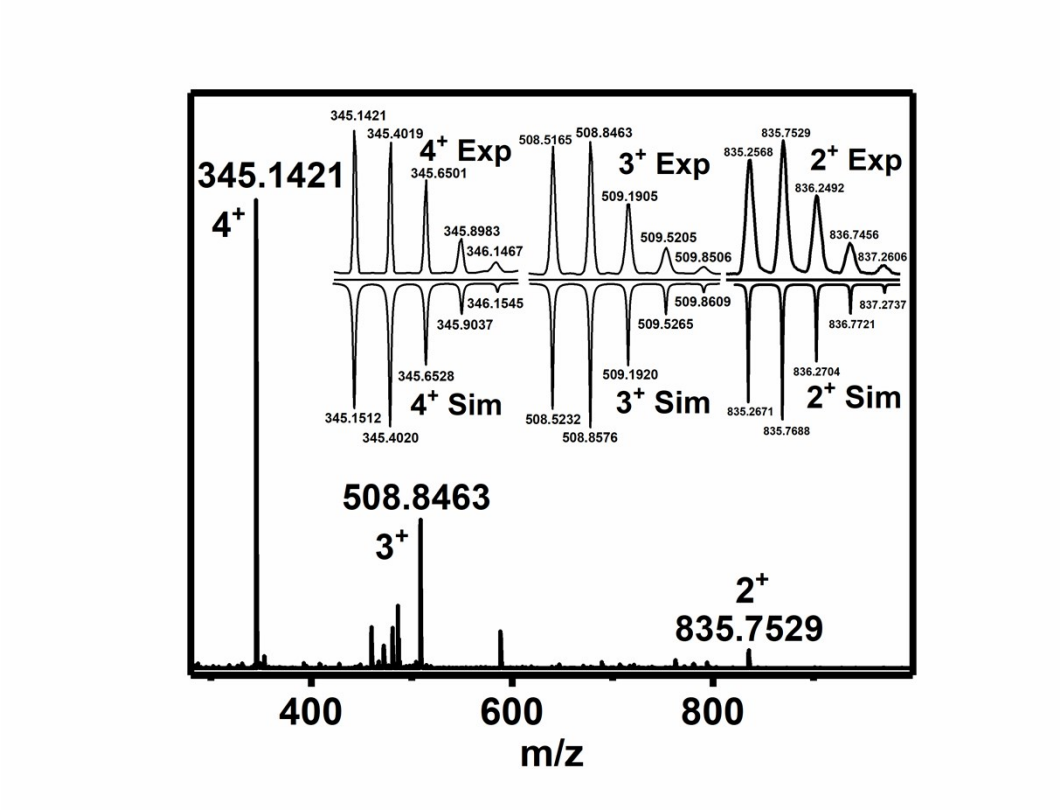

Figure S15. Experimental and calculated electrospray ionization mass spectra of **2**•4PF_6^-.

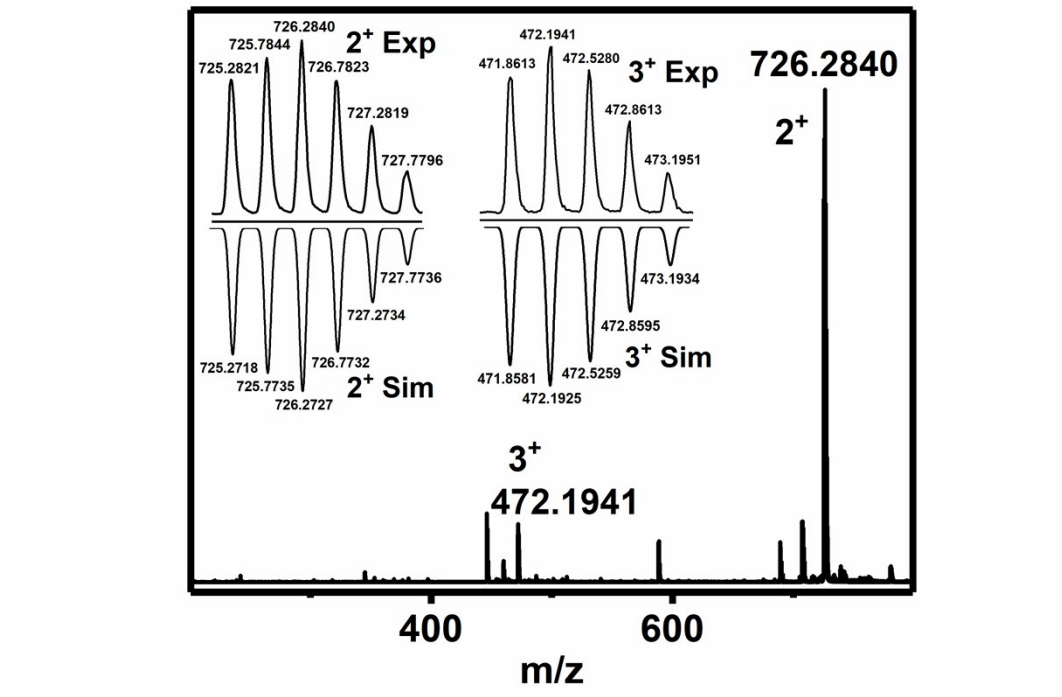

Figure S16. Experimental and calculated electrospray ionization mass spectra of **2**•4Cl^-.

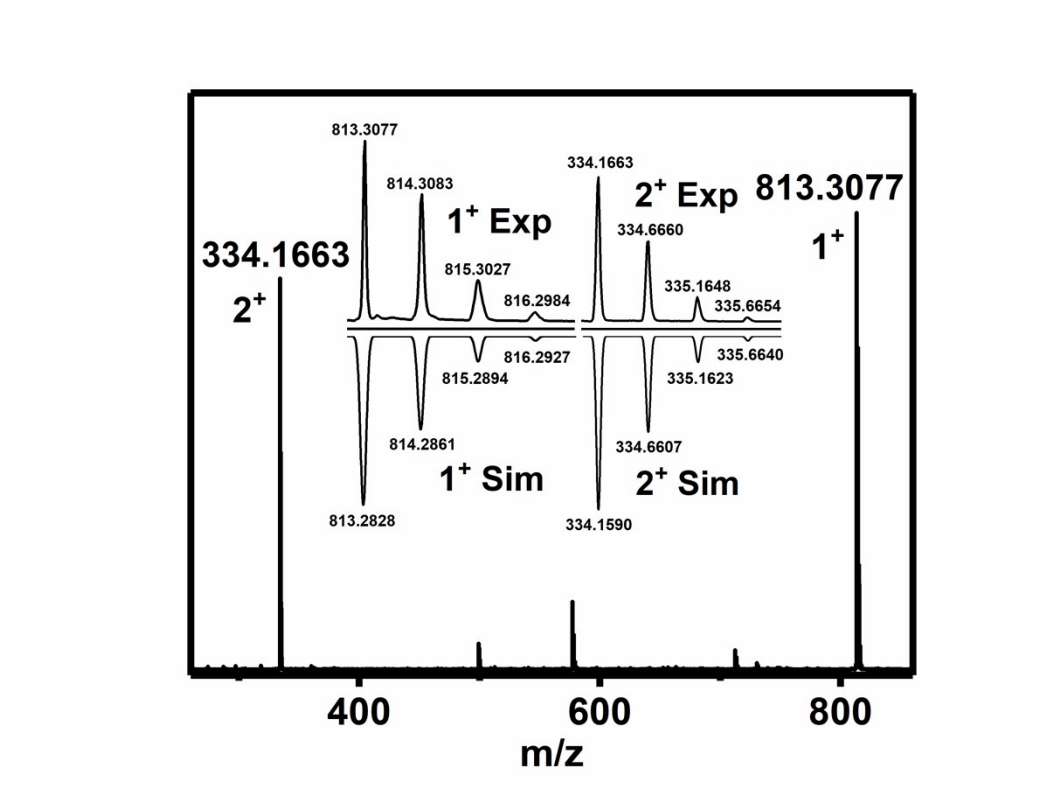

Figure S17. Experimental and calculated electrospray ionization mass spectra of **3**•2PF_6^-.

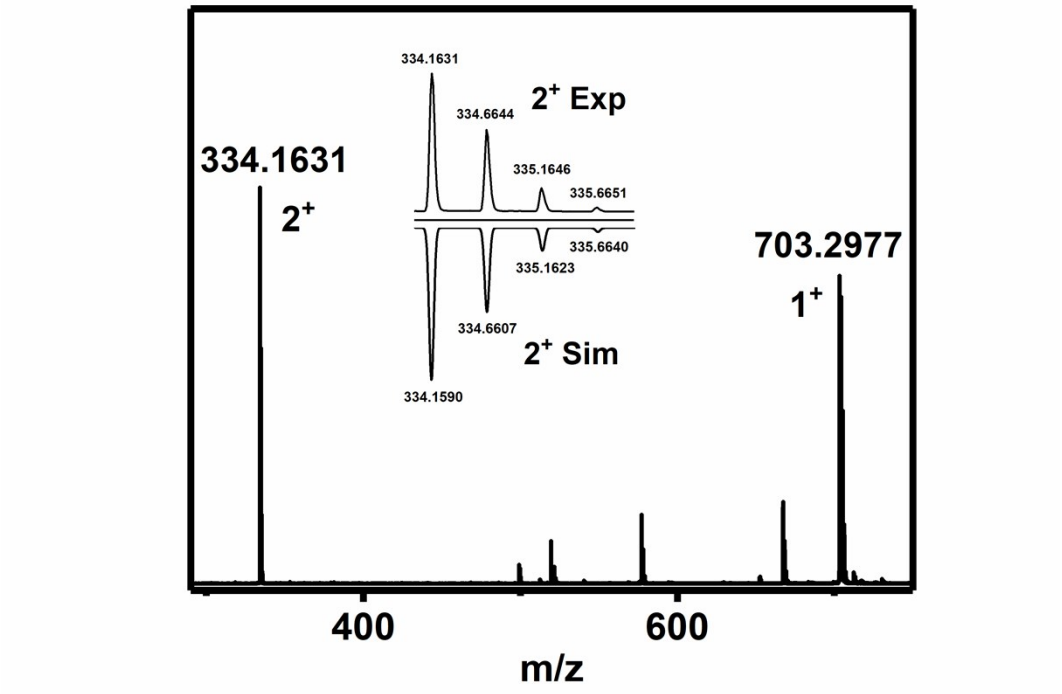

Figure S18. Experimental and calculated electrospray ionization mass spectra of **3**•2Cl^-.

X-ray Structure determination.

The crystal of **1**•4PF_6^-: Data collections was performed on Bruker VENTURE system with PHOTON 100 CMOS detector equipped and a Ga-target Liquid METALJET D2 PLUS X-ray Source (λ = 1.34139 Å). The data was collected at 180 K crystal temperature (Oxford Cryosystems CRYOSTREAM 700), 50 kV and 30 mA with an appropriate 0.5° ω and φ scan strategy. Data reduction and integration were performed with SAINT (version 8.38A).[1] Data was corrected for absorption effects using the empirical methods as implemented in SADABS (version 2016/2).[2] The structure was solved by SHELXT (version 2018/2)[3] and refined by full-matrix least-squares procedures using the SHELXL program (version 2018/3)[4] through the OLEX2[5] graphical interface. All non-hydrogen atoms, including those in disordered parts, were refined anisotropically. All H-atoms were included at calculated positions and refined as riders, with Uiso(H) = 1.2 Ueq(C). In each unit cell, there are 20 acetonitrile molecules that were found to be severely disordered and removed by the SQUEEZE routine in PLATON (version 220719).[6] Further crystal and data collection details are listed in Table S1.

1•4PF_6^- was dissolved in MeCN and the solution was passed through a 0.10 μm filter into a 10 mL tube, which was placed inside a 500 mL wild-mouth bottle containing isopropyl ether (50 mL). The bottle was capped, after slow evaporation of diethyl ether at 4℃ into the MeCN solution for 14 days, and light-yellow single crystals of **1**•4PF_6^- were obtained.

Table S1. Crystal data and structure refinement for **1•4**PF_6^-.

Chemical formula	$C_{98}H_{83}N_9P_4F_{24}$
M_r	1966.61
Crystal system, space group	Monoclinic, P 2_1/c
Temperature (K)	150
a, *b*, *c* (Å)	22.092(3), 20.054(3), 42.684(6)
α, *β*, *γ* (°)	90, 97.443(5), 90

V (Å^3)	18751(4)
Z	8
F(000)	8080.0
D_x (Mg m^{-3})	1.393
Radiation type	Ga Kα, λ= 1.34138 Å
μ (mm^{-1})	1.042
Crystal size (mm)	0.3 × 0.3 × 0.2
Diffractometer	Bruker D8 Venture PHOTON 100 CMOS
Radiation source	Liquid METALJET D2 PLUS X-ray Source
Scan method	ϕ and ω scans
Absorption correction	Multi-scan SADABS2016/2 (Bruker,2016/2) was used for absorption correction.
T_{min}, T_{max}	0.586, 0.751
No. of measured, independent and observed [$I > 2^{\sigma}(I)$] reflections	396547 , 33096, 25994
R_{int}	0.059
θ values (°)	θ_{max} = 53.0, θ_{min} = 2.1
(sin $\theta/\lambda)_{max}$ (Å^{-1})	0.998
Range of h, k, l	h = -26→26, k = -23→23, l = -50→50
$R[F^2 > 2\sigma(F^2)]$, $wR(F^2)$, S	0.083 , 0.245, 1.03
No. of reflections	33096
No. of parameters	2404
No. of restraints	366
$\Delta>_{max}$, $\Delta>_{min}$ (e Å^{-3})	1.50, -0.71

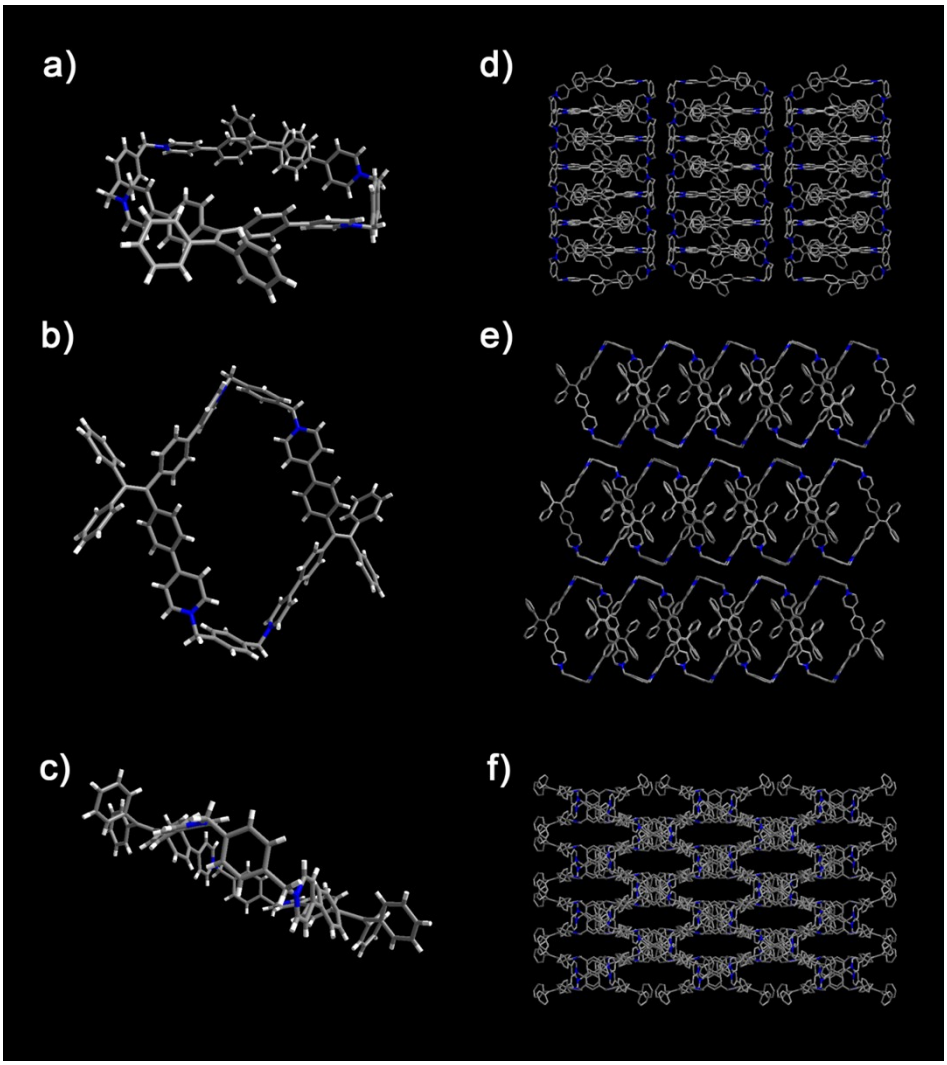

Figure S19. Solid-state (super)structures of cyclophane **1**•4PF_6^- obtained from single crystal X-ray crystallography. a) a axis, b) b axis and c) c axis of cyclophane **1**•4PF_6^-. d) a axis, e) b axis and f) c axis of molecular packing of cyclophane **1**•4PF_6^-. Color code: N, blue; C, gray; H, white. The solvent molecules and PF_6^- pairsare omitted.

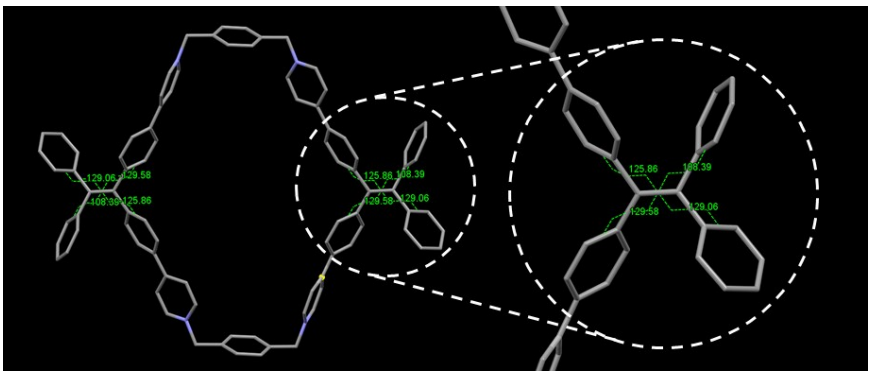

Figure S20. The torsion angles four benzene rings of TPE in **1•4**PF_6^-.

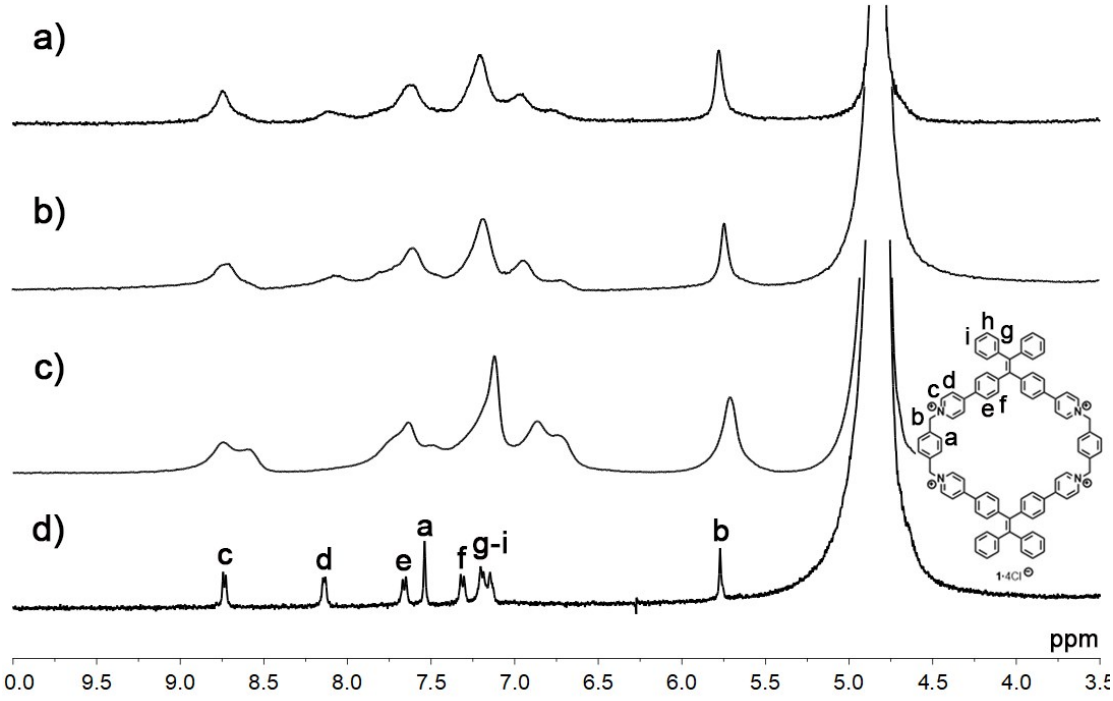

Figure S21. ^{1}H NMR spectrum recorded (400 MHz, D_2O, RT) for **1**•4Cl^{-} of a) 5.0mM, b) 1.0mM, c) 0.4mM, d) 0.2mM.

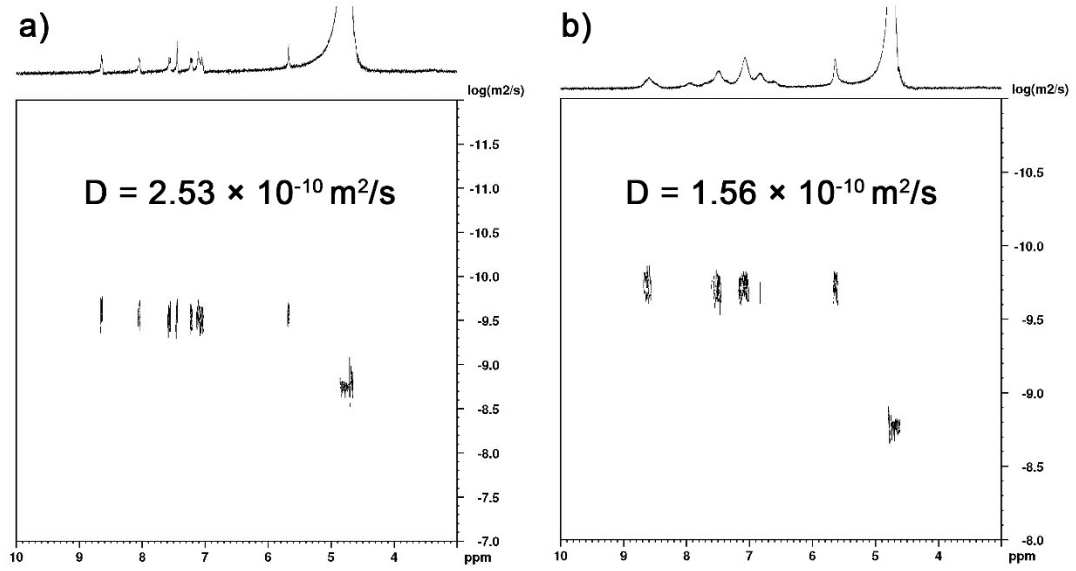

Figure S22. 2D DOSY spectra (400 MHz, D_2O, RT) for **1**•4Cl^{-} of a) 0.2mM, b) 1.0mM.

UV/vis and fluorescence titration experiments

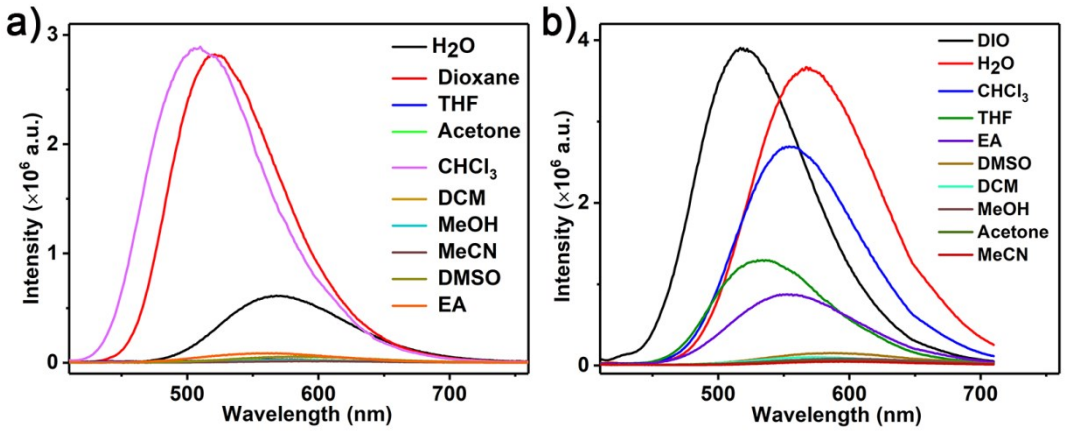

Figure S23. Fluorescence spectra of (a) **1**•4PF_6^- (10 μM), (b)**2**•4PF_6^- (10 μM) in different solvents (1% MeCN). (a) λ_{ex} = 390 nm, (b) λ_{ex} = 365 nm, Ex/Em slit = 3 nm.

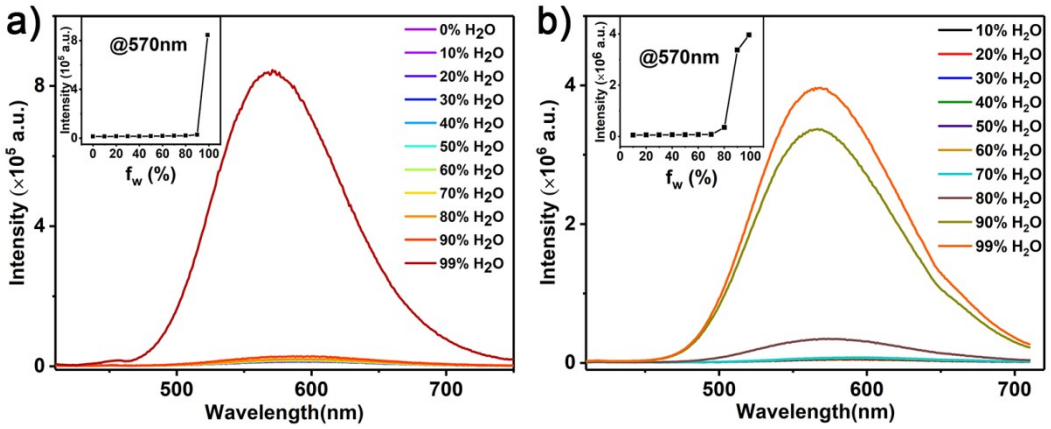

Figure S24. Fluorescence spectra and plot of maximum emission intensity of (a) **1**•4PF_6^- (10 μM), (b) **2**•4PF_6^- (10 μM) versus water fraction in MeCN-water mixture. (a) λ_{ex} = 390 nm, (b) λ_{ex} = 365 nm, Ex/Em slit = 3 nm.

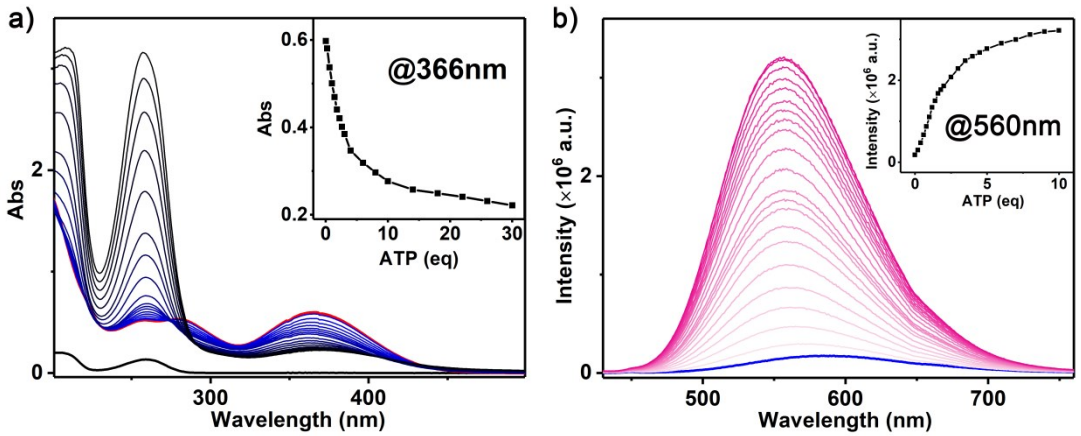

Figure S25. (a) UV-vis absorption and (b) fluorescence spectra of **1**•4Cl$^-$ (10 μM) in water upon addition of ATP. λ_{ex} = 390 nm, Ex/Em slit = 3 nm.

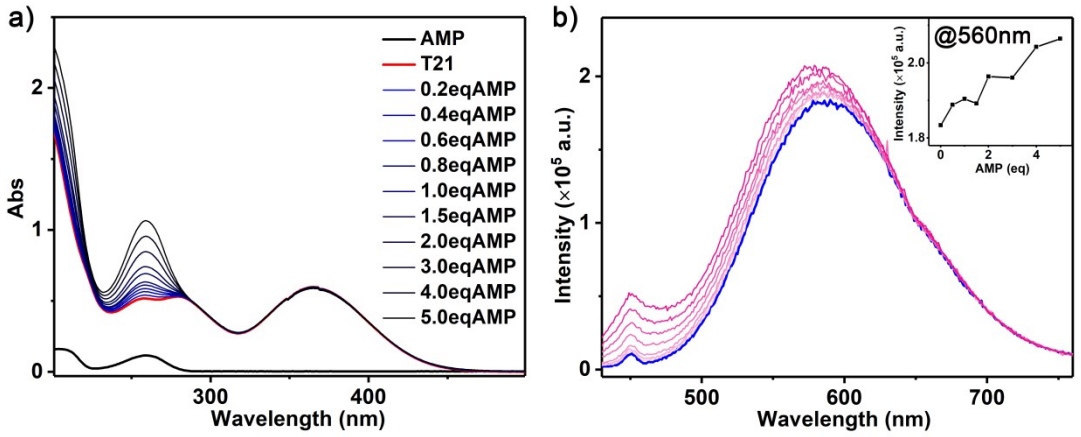

Figure S26. (a) UV-vis absorption and (b) fluorescence spectra of **1**•4Cl$^-$ (10 μM) in water upon addition of AMP. λ_{ex} = 390 nm, Ex/Em slit = 3 nm.

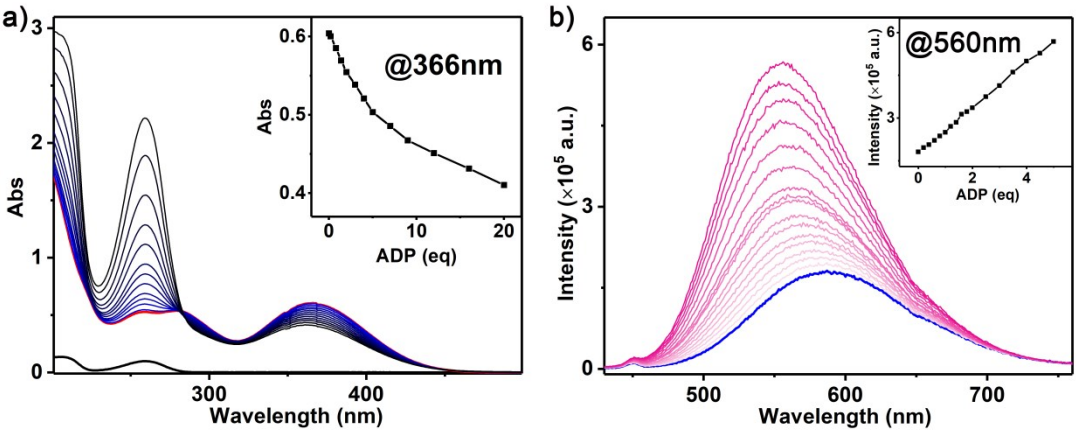

Figure S27. (a) UV-vis absorption and (b) fluorescence spectra of **1**•4Cl$^-$ (10 μM) in water upon addition of ADP. λ_{ex} = 390 nm, Ex/Em slit = 3 nm.

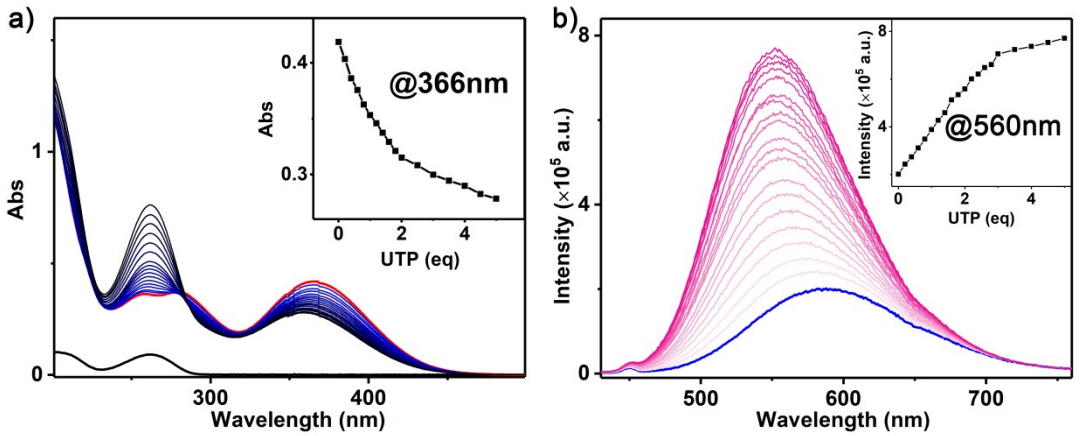

Figure S28. (a) UV-vis absorption and (b) fluorescence spectra of **1**•4Cl^{-} (10 μM) in water upon addition of UTP. λ_{ex} = 390 nm, Ex/Em slit = 3 nm.

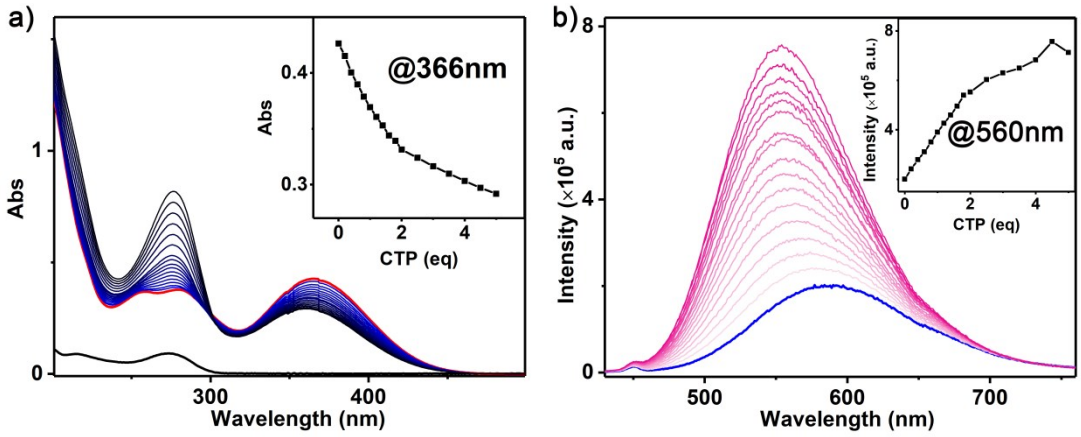

Figure S29. (a) UV-vis absorption and (b) fluorescence spectra of **1**•4Cl^{-} (10 μM) in water upon addition of CTP. λ_{ex} = 390 nm, Ex/Em slit = 3 nm.

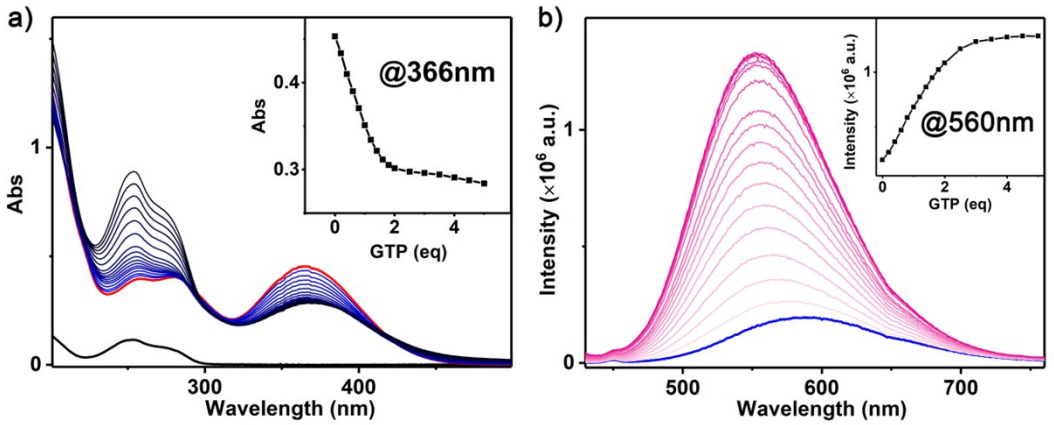

Figure S30. (a) UV-vis absorption and (b) fluorescence spectra of **1**•4Cl^{-} (10 μM) in water upon addition of GTP. λ_{ex} = 390 nm, Ex/Em slit = 3 nm.

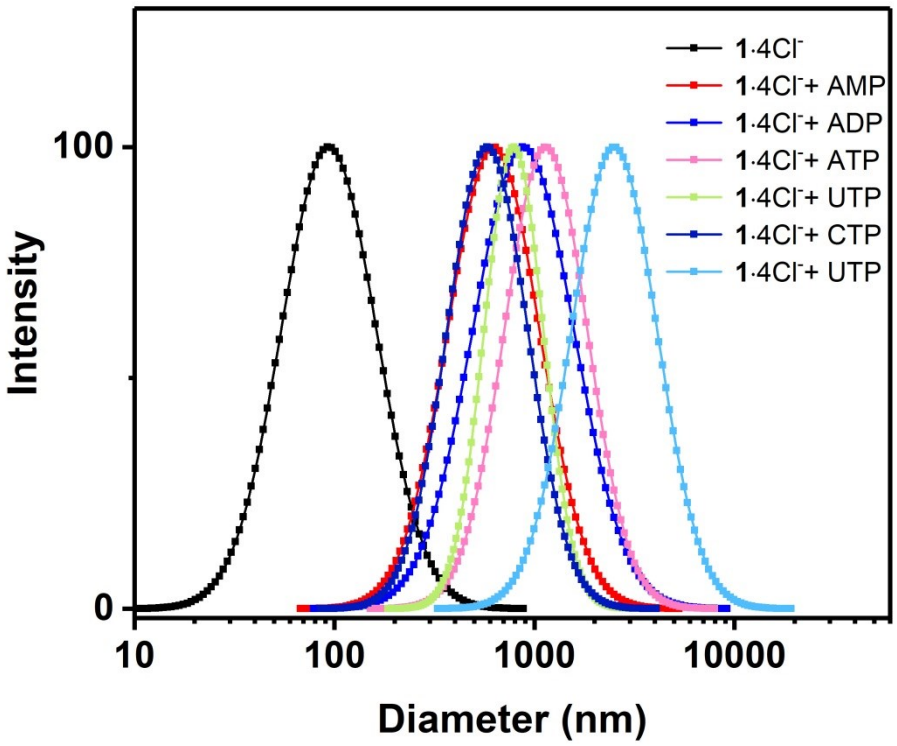

Compound	Diameter (nm)
1•4Cl¯	94.5 ± 0.9
1•4Cl¯□AMP	626.0 ± 67.7
1•4Cl¯□ADP	880.4 ± 57.6
1•4Cl¯□ATP	1166.2 ± 95.7
1•4Cl¯□UTP	800.5 ± 45.3
1•4Cl¯□CTP	581.0 ± 7.8
1•4Cl¯□GTP	2534.1 ± 311.3

Fig S31. DLS profiles of **1**•4Cl¯ (10 μM) with nucleotides (5.0 equiv) in water.

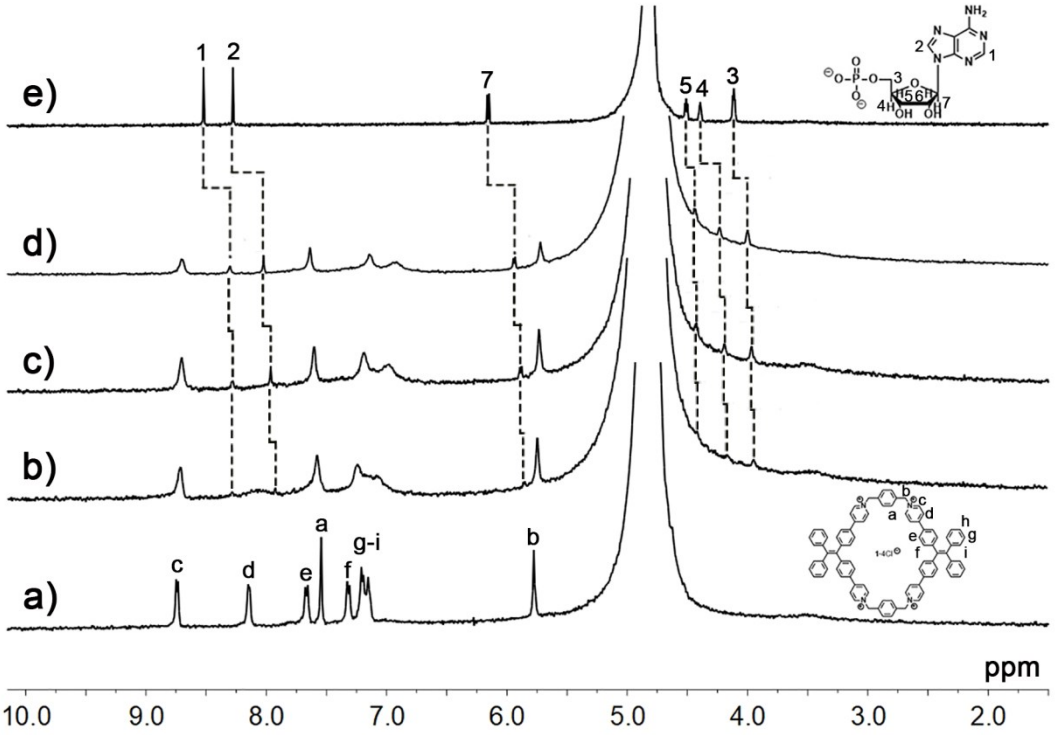

Figure S32. ^{1}H NMR spectra (400MHz, D_2O, 298K) recorded for: a) **1**•4Cl^{-}; b) **1**•4Cl^{-} and AMP (0.5 eq.); c) **1**•4Cl^{-} and AMP (1.0 eq.); d) **1**•4Cl^{-} and AMP (2.0 eq.); e) AMP.

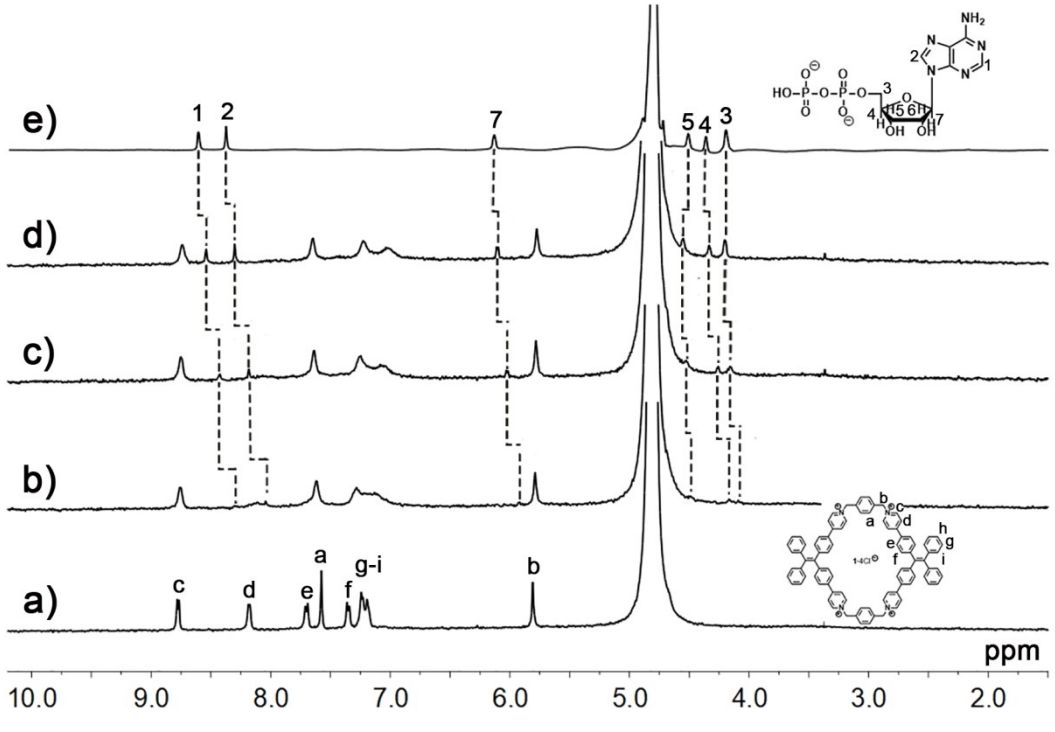

Figure S33. ^{1}H NMR spectra (400MHz, D_2O, 298K) recorded for: a) **1**•4Cl^{-}; b) **1**•4Cl^{-}

and ADP (0.5 eq.); c) **1**•4Cl$^-$ and ADP (1.0 eq.); d) **1**•4Cl$^-$ and ADP (2.0 eq.); e) ADP.

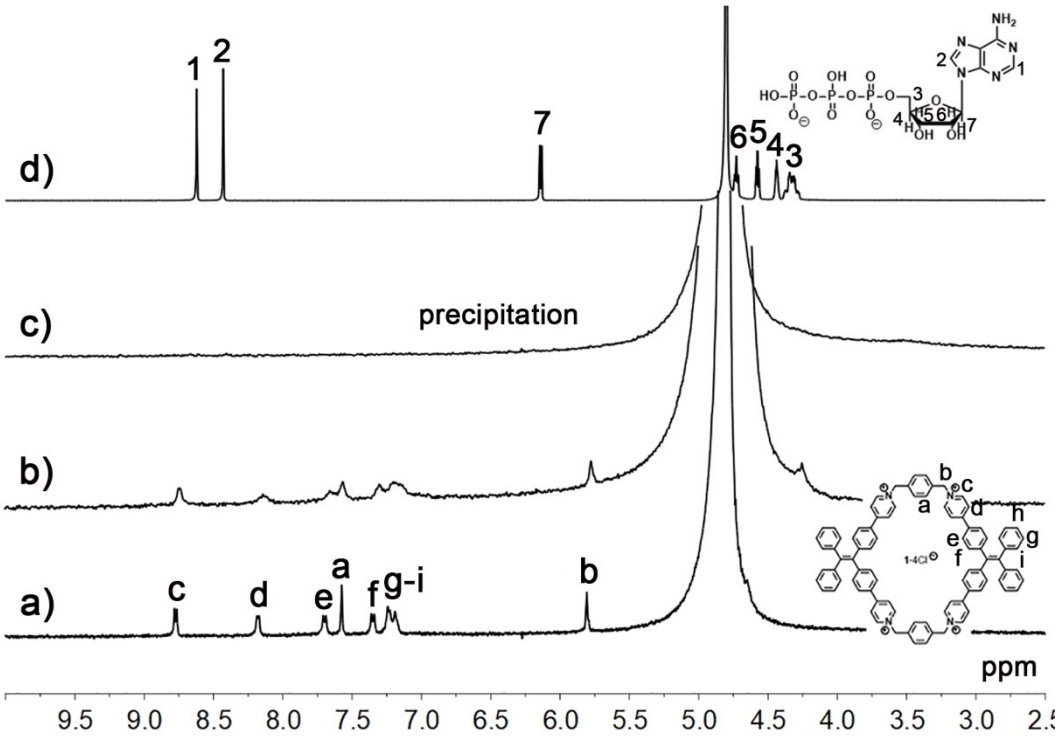

Figure S34. ^{1}H NMR spectra (400MHz, D_2O, 298K) recorded for: a) **1**•4Cl$^-$; b) **1**•4Cl$^-$ and ATP (1.0 eq.); d) **1**•4Cl$^-$ and ATP (2.0 eq.); e) ATP.

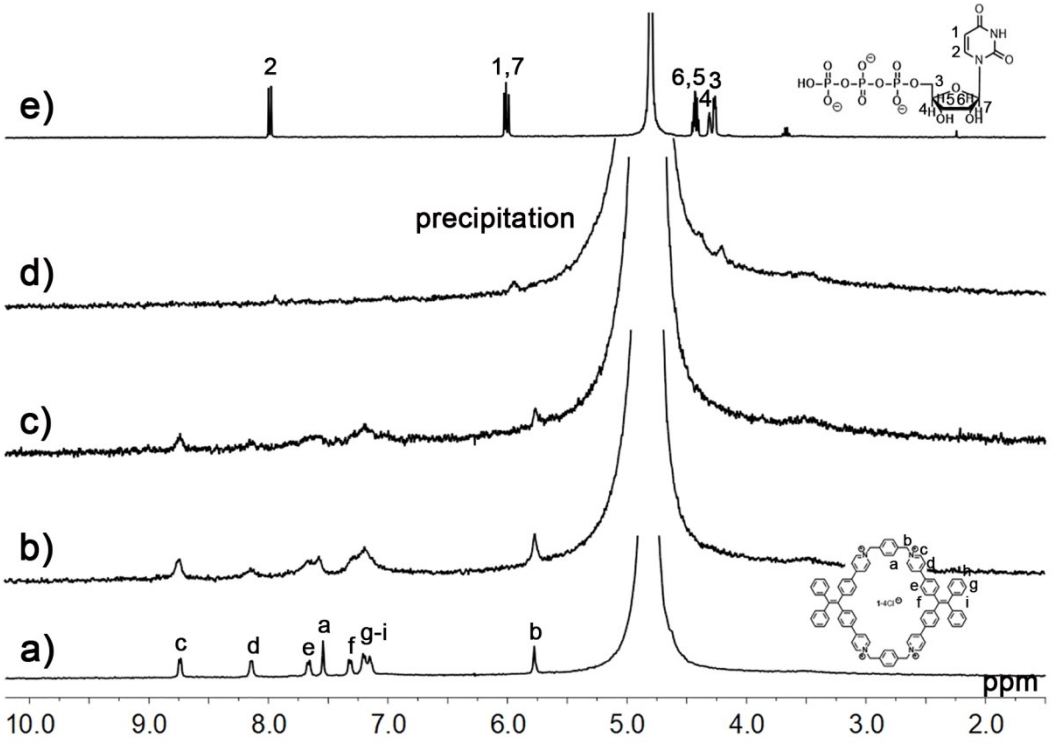

Figure S35. ^{1}H NMR spectra (400MHz, D_2O, 298K) recorded for: a) **1**•4Cl$^-$; b) **1**•4Cl$^-$

and UTP (0.5 eq.); c) **1**•4Cl$^-$ and UTP (1.0 eq.); d) **1**•4Cl$^-$ and UTP (2.0 eq.); e) UTP.

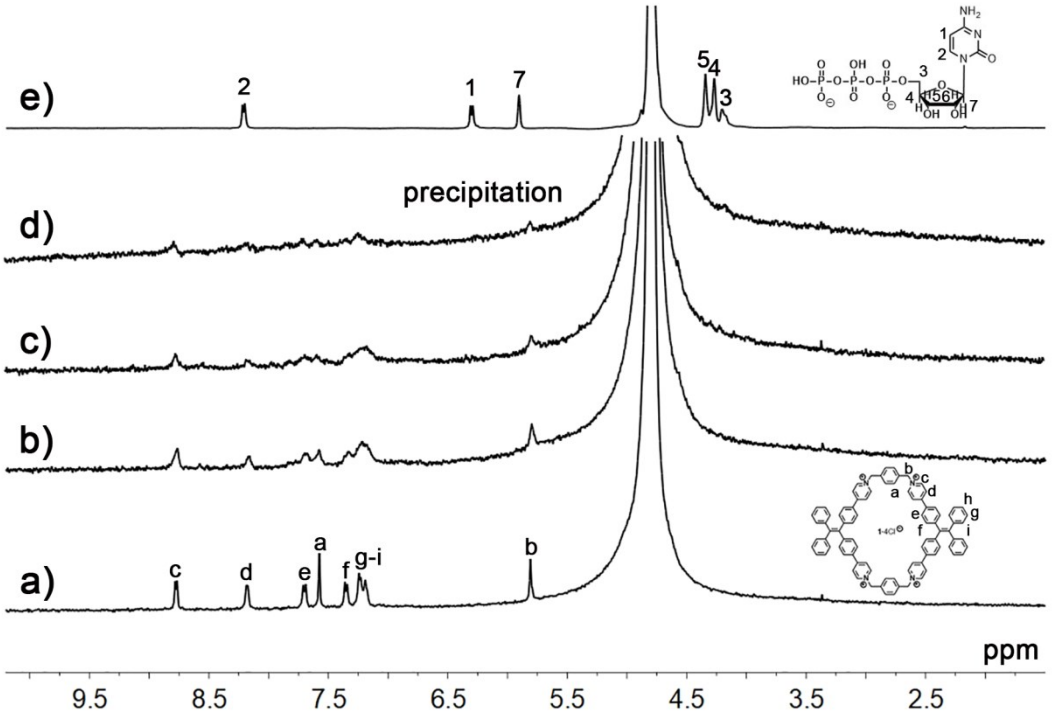

Figure S36. ^{1}H NMR spectra (400MHz, D_2O, 298K) recorded for: a) **1**•4Cl$^-$; b) **1**•4Cl$^-$ and CTP (0.5 eq.); c) **1**•4Cl$^-$ and CTP (1.0 eq.); d) **1**•4Cl$^-$ and CTP (2.0 eq.); e) CTP.

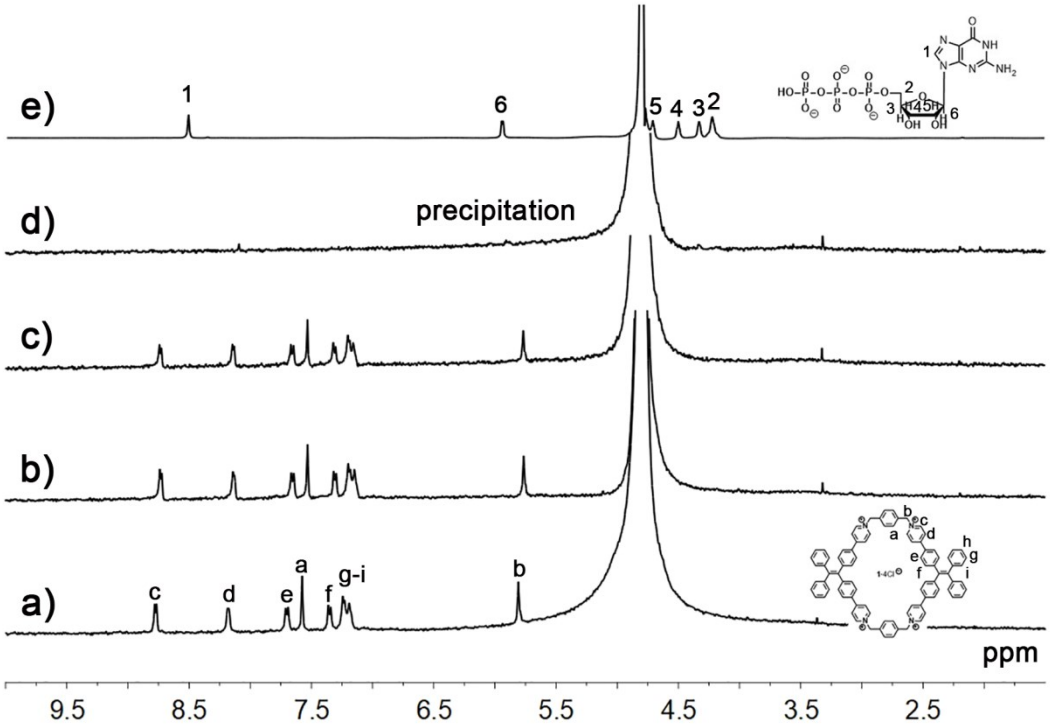

Figure S37. ^{1}H NMR spectra (400MHz, D_2O, 298K) recorded for: a) **1**•4Cl$^-$; b) **1**•4Cl$^-$

and GTP (0.5 eq.); c) **1**•4Cl^{-} and GTP (1.0 eq.); d) **1**•4Cl^{-} and GTP (2.0 eq.); e) GTP.

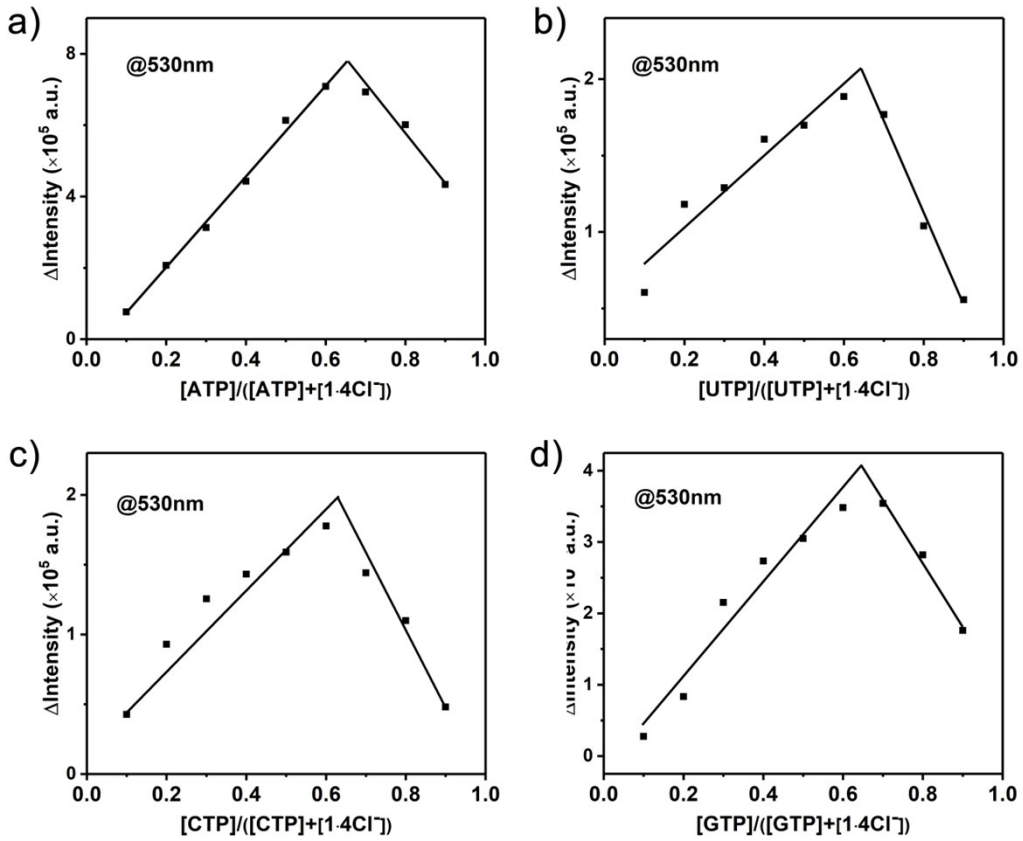

Figure S38. Job's plots obtained by recording the fluorescence at 530 nm for the solution of a) **1**•4Cl^{-} and ATP ([**1**•4Cl^{-}]+[ATP] = 10 μM) , b) **1**•4Cl^{-} and UTP ([**1**•4Cl^{-}]+[UTP] = 10 μM) , c) **1**•4Cl^{-} and CTP ([**1**•4Cl^{-}]+[CTP] = 10 μM) , d) **1**•4Cl^{-} and GTP ([**1**•4Cl^{-}]+[GTP] = 10 μM) in water at RT, confirming the 1:2 stoichiometry of both complexes. λ_{ex} = 390 nm, Ex/Em slit = 3 nm.

Table S2. Absolute quantum yield (Φ_F), fluorescence intensity ratio (I/I_0), and apparent binding constants of **1**•4Cl$^-$ for various guests.

	Φ_F (%)		I/I_0			K_a^*($\times 10^6$ M^{-1})
Host / **Guest**	**1**•4Cl$^-$	**2**•4Cl$^-$	**1**•4Cl$^-$	**2**•4Cl$^-$	**3**•2Cl$^-$	**1**•4Cl$^-$
None	0.05	–	1	1	1	–
AMP	–	0.23	1.13	1.24	0.99	–
ADP	12.42	4.57	3.13	3.33	1.01	7.70 ± 0.31
ATP	19.19	5.11	15.76	6.42	1.06	23.3 ± 1.3
UTP	11.24	4.69	3.83	5.87	0.98	9.85 ± 0.61
CTP	11.82	4.77	3.55	4.83	0.99	12.8 ± 0.8
GTP	2.14	1.42	6.80	2.60	0.96	2.51 ± 0.40
smDNA	9.03	2.88	21.48	6.01	–	–
ctDNA	6.67	4.70	20.66	6.09	–	–

[a]The change of UV-vis absorption after the addition of guest to the **1**•4Cl$^-$ was calculated K_a by using Dynafit program.

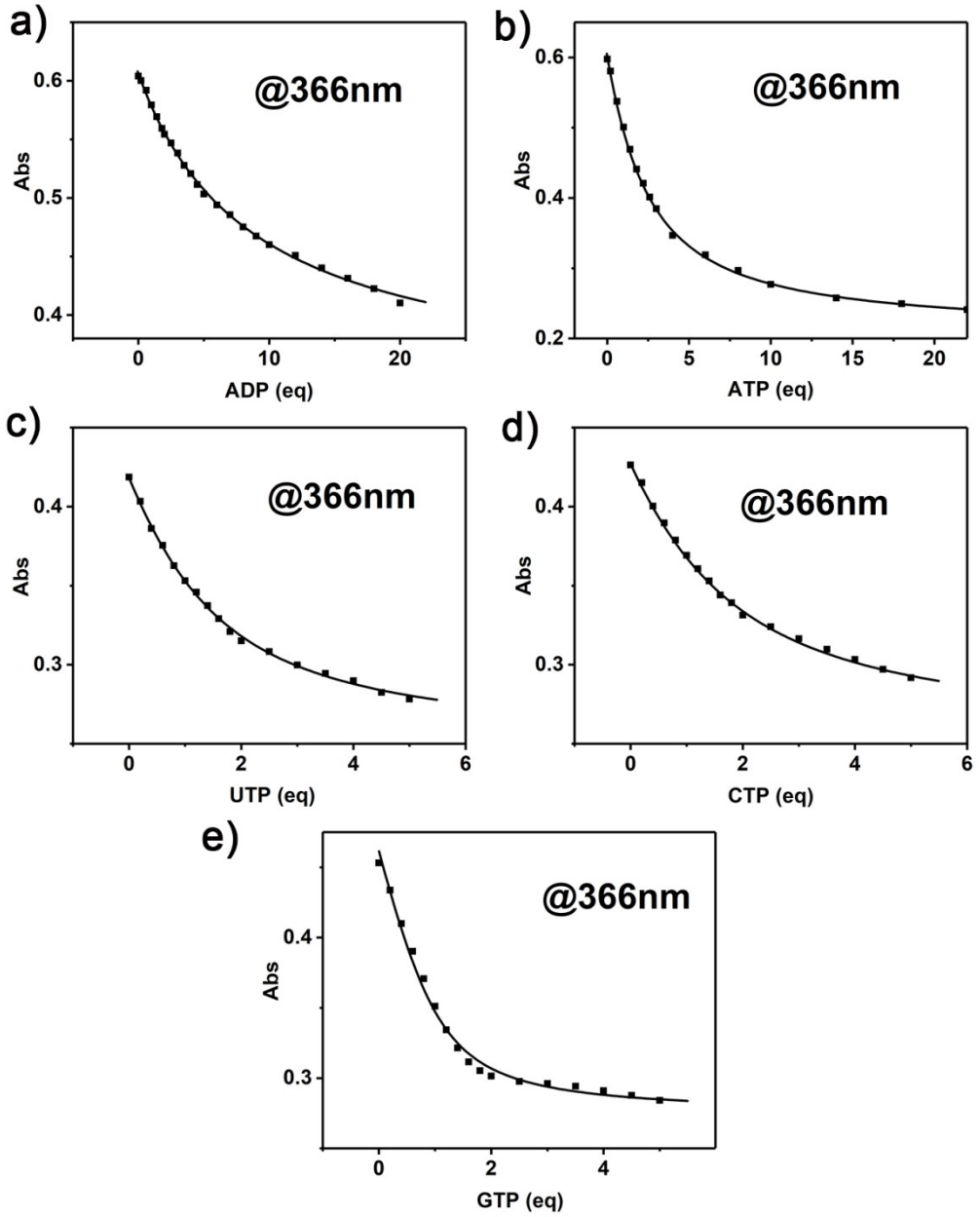

Figure S39. Non-linear fitting curve of the UV-vis absorption changes of **1**•4Cl^- versus the concentration of (a) ADP, (b) ATP, (c) UTP, (d) CTP, (e) GTP.

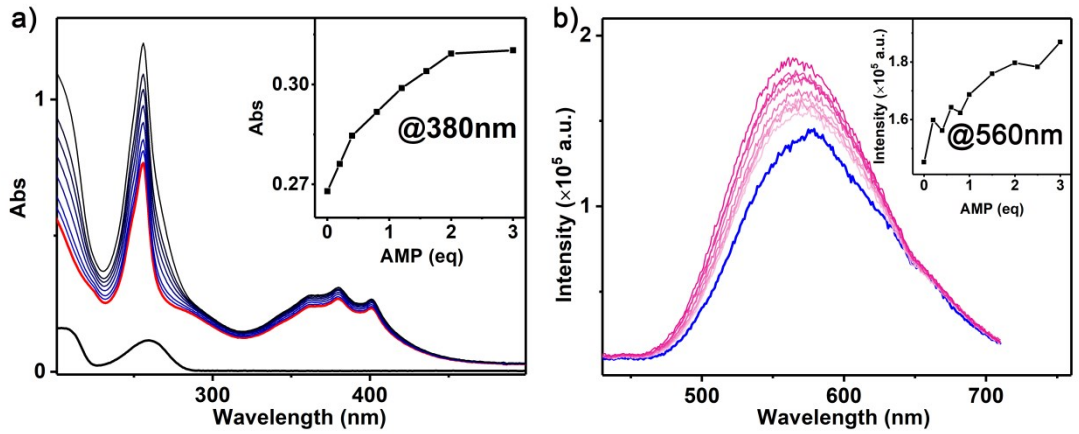

Figure 40. (a) UV-vis absorption and (b) fluorescence spectra of **2**•4Cl^{-} (10 μM) in water upon addition of AMP. λ_{ex} = 365 nm, Ex/Em slit = 3 nm.

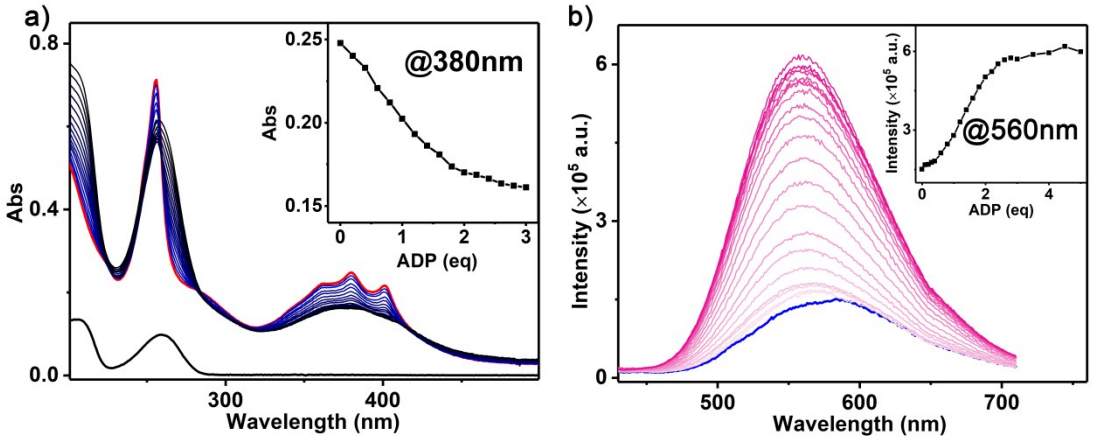

Figure S41. (a) UV-vis absorption and (b) fluorescence spectra of **2**•4Cl^{-} (10 μM) in water upon addition of ADP. λ_{ex} = 365 nm, Ex/Em slit = 3 nm.

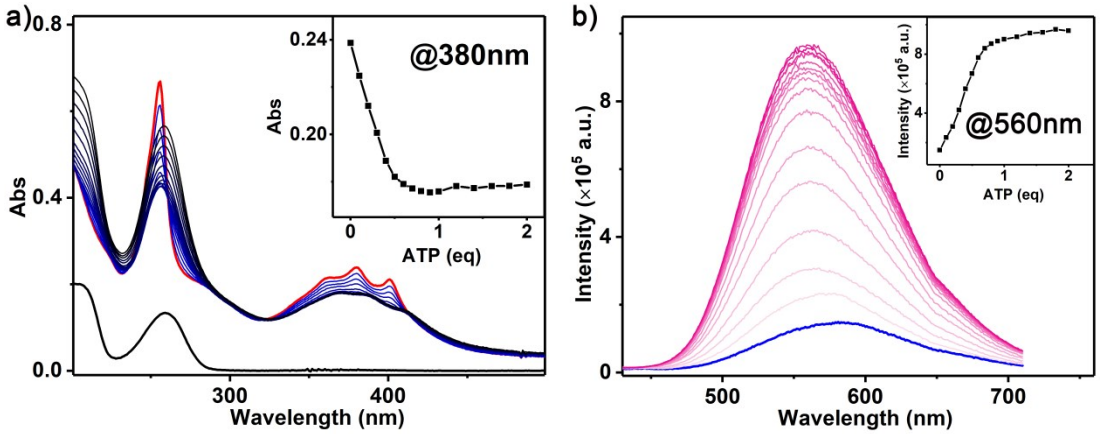

Figure S42. (a) UV-vis absorption and (b) fluorescence spectra of **2**•4Cl^{-} (10 μM) in water upon addition of ATP. λ_{ex} = 365 nm, Ex/Em slit = 3 nm.

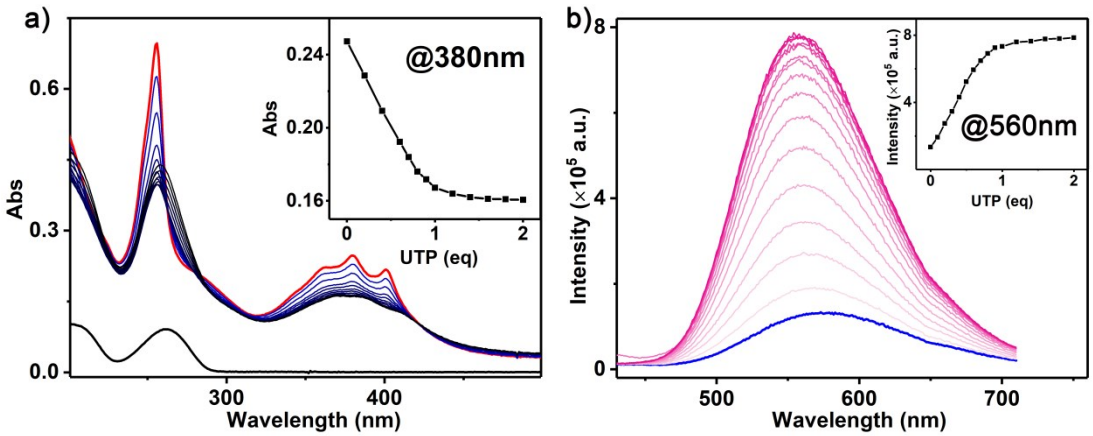

Figure S43. (a) UV-vis absorption and (b) fluorescence spectra of **2**•4Cl^{-} (10 μM) in water upon addition of UTP. λ_{ex} = 365 nm, Ex/Em slit = 3 nm.

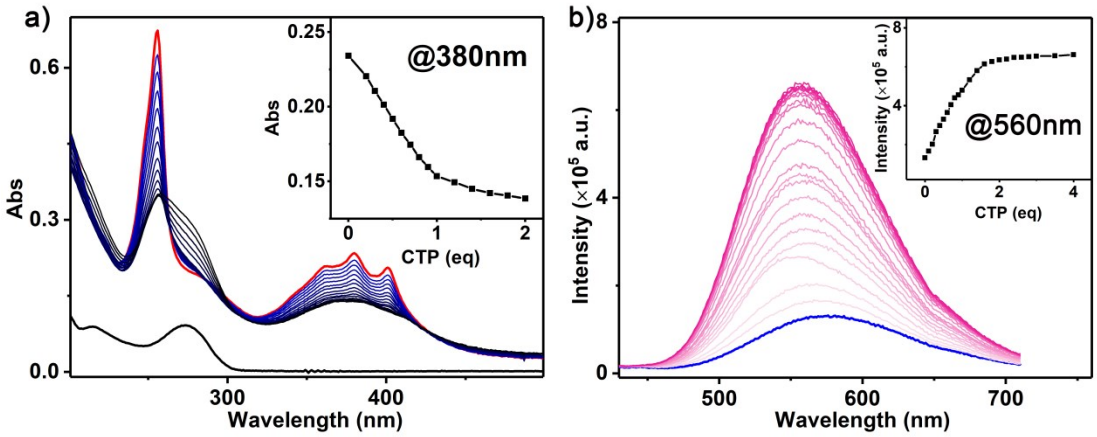

Figure S44. (a) UV-vis absorption and (b) fluorescence spectra of **2**•4Cl^{-} (10 μM) in water upon addition of CTP. λ_{ex} = 365 nm, Ex/Em slit = 3 nm.

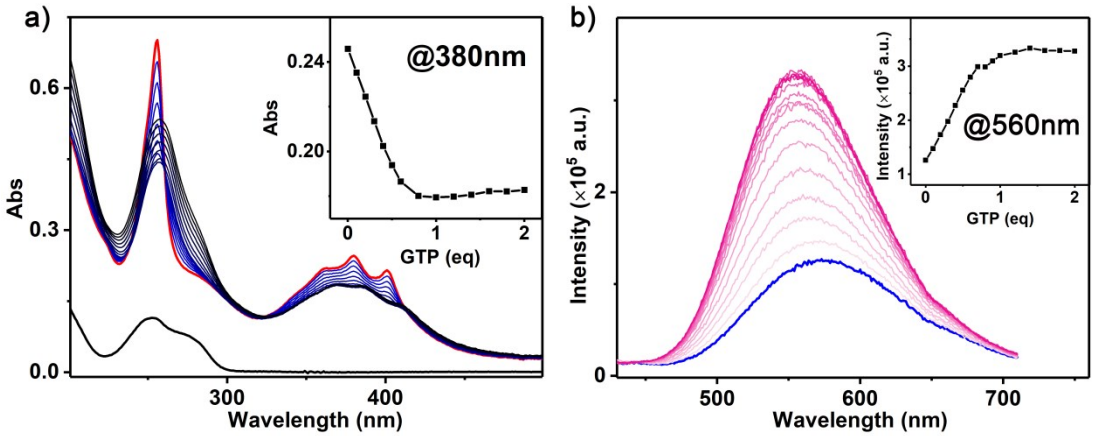

Figure S45. (a) UV-vis absorption and (b) fluorescence spectra of **2**•4Cl^{-} (10 μM) in water upon addition of GTP. λ_{ex} = 365 nm, Ex/Em slit = 3 nm.

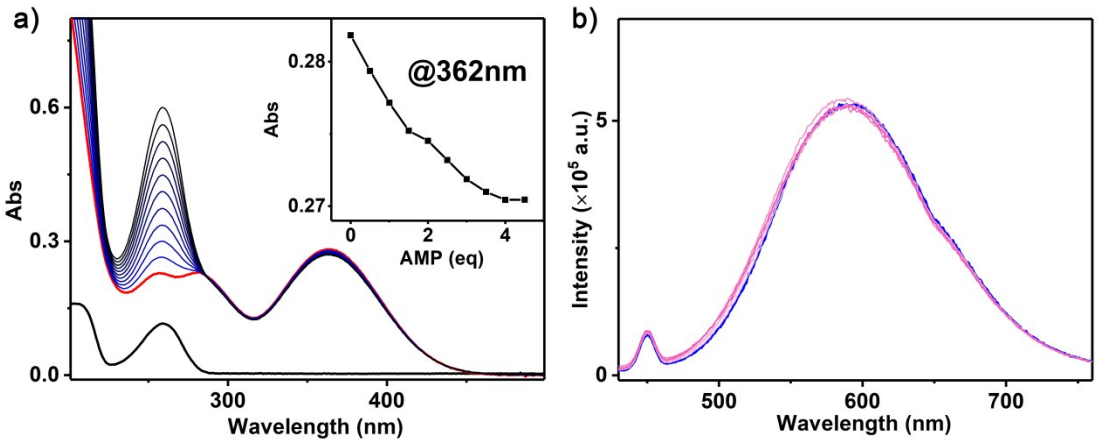

Figure S46. (a) UV-vis absorption and (b) fluorescence spectra of **3**•2Cl^{-} (10 μM) in water upon addition of AMP. λ_{ex} = 395 nm, Ex/Em slit = 3 nm.

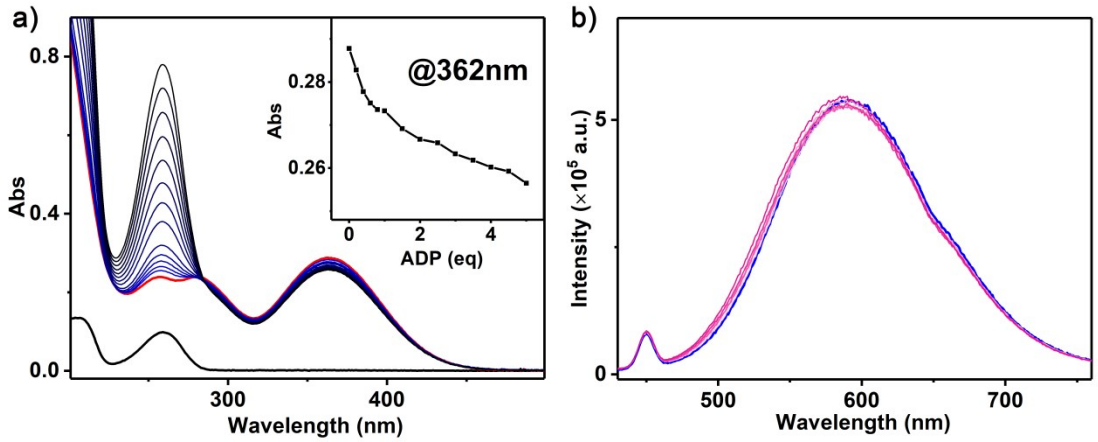

Figure S47. (a) UV-vis absorption and (b) fluorescence spectra of **3**•2Cl^{-} (10 μM) in water upon addition of ADP. λ_{ex} = 395 nm, Ex/Em slit = 3 nm.

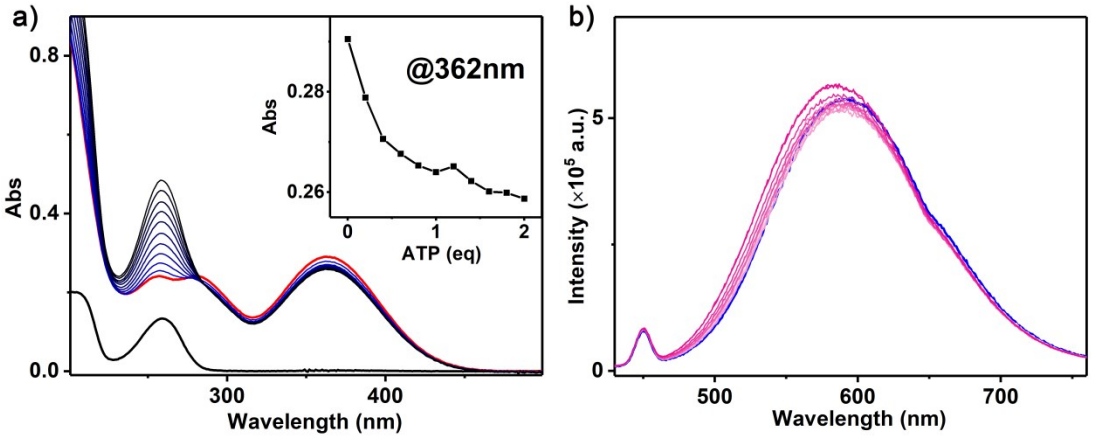

Figure S48. (a) UV-vis absorption and (b) fluorescence spectra of **3**•2Cl^{-} (10 μM) in water upon addition of ATP. λ_{ex} = 395 nm, Ex/Em slit = 3 nm.

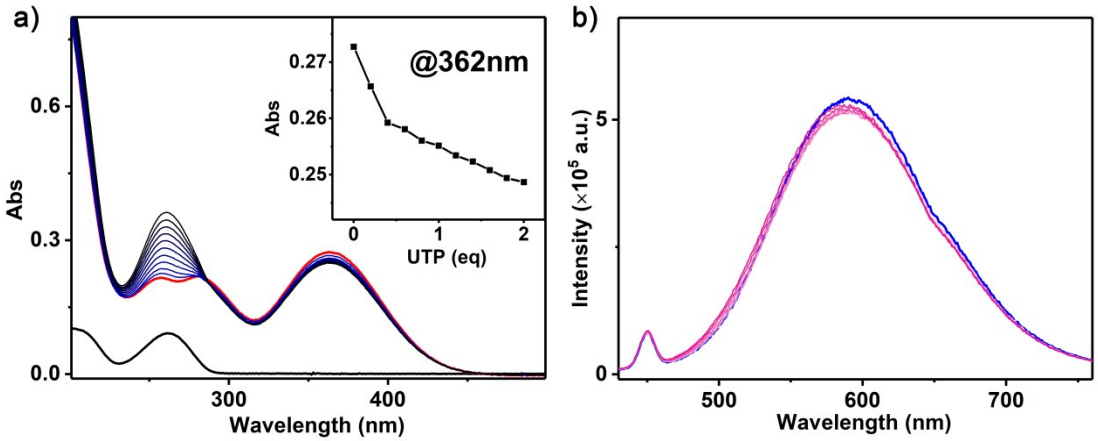

Figure S49. (a) UV-vis absorption and (b) fluorescence spectra of **3**•2Cl$^-$ (10 μM) in water upon addition of UTP. λ_{ex} = 395 nm, Ex/Em slit = 3 nm.

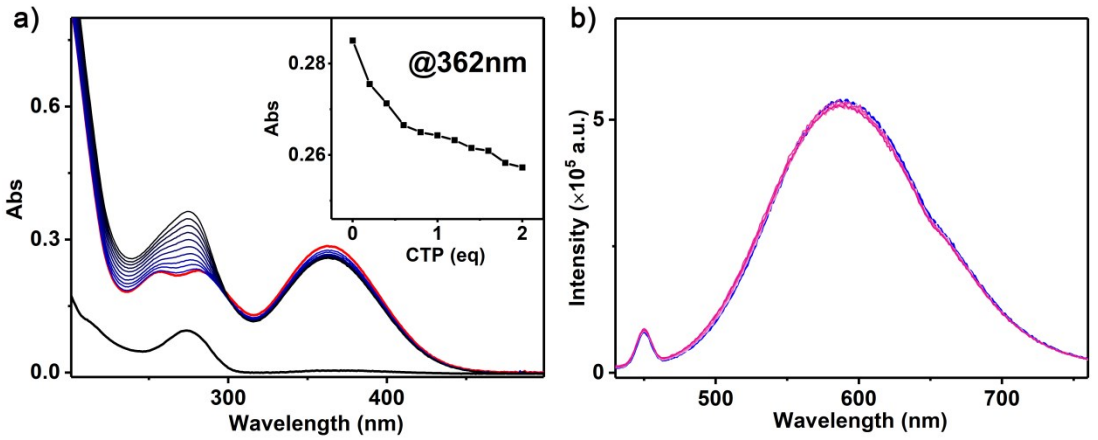

Figure S50. (a) UV-vis absorption and (b) fluorescence spectra of **3**•2Cl$^-$ (10 μM) in water upon addition of CTP. λ_{ex} = 395 nm, Ex/Em slit = 3 nm.

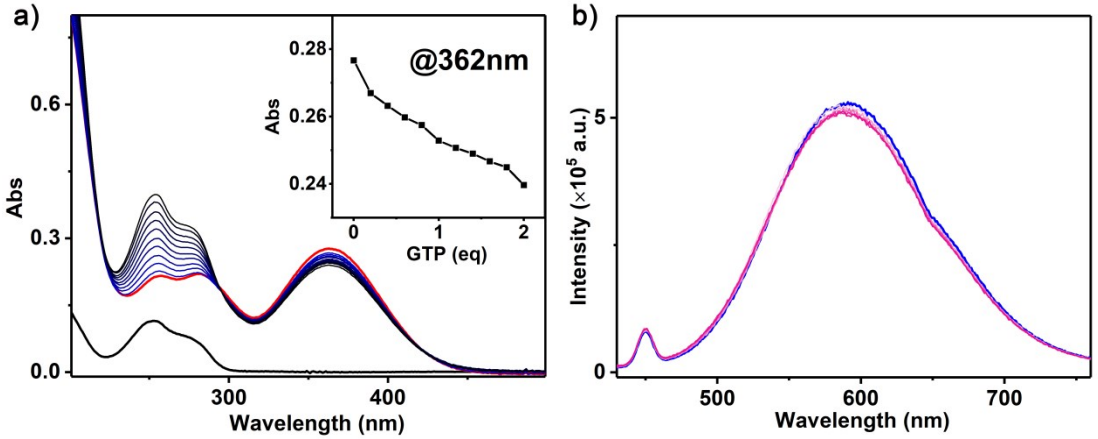

Figure S51. (a) UV-vis absorption and (b) fluorescence spectra of **3**•2Cl$^-$ (10 μM) in water upon addition of GTP. λ_{ex} = 395 nm, Ex/Em slit = 3 nm.

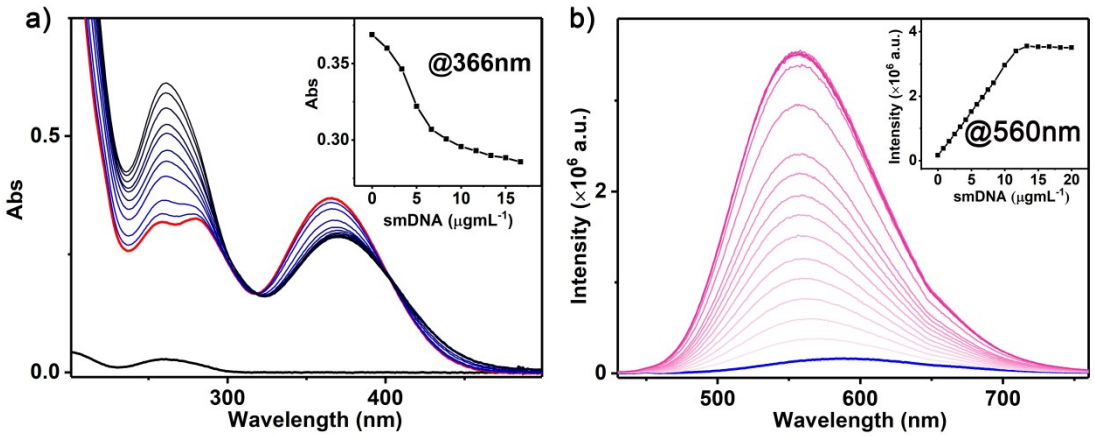

Figure S52. (a) UV-vis absorption and (b) fluorescence spectra of **1**•4Cl^{-} (10 μM) in water upon addition of smDNA. λ_{ex} = 390 nm, Ex/Em slit = 3 nm.

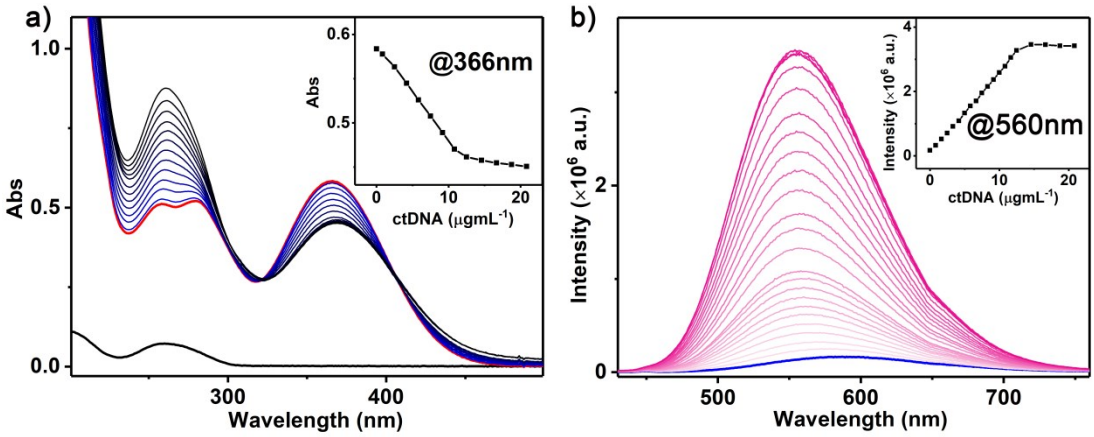

Figure S53. (a) UV-vis absorption and (b) fluorescence spectra of **1**•4Cl^{-} (10 μM) in water upon addition of ctDNA. λ_{ex} = 390 nm, Ex/Em slit = 3 nm.

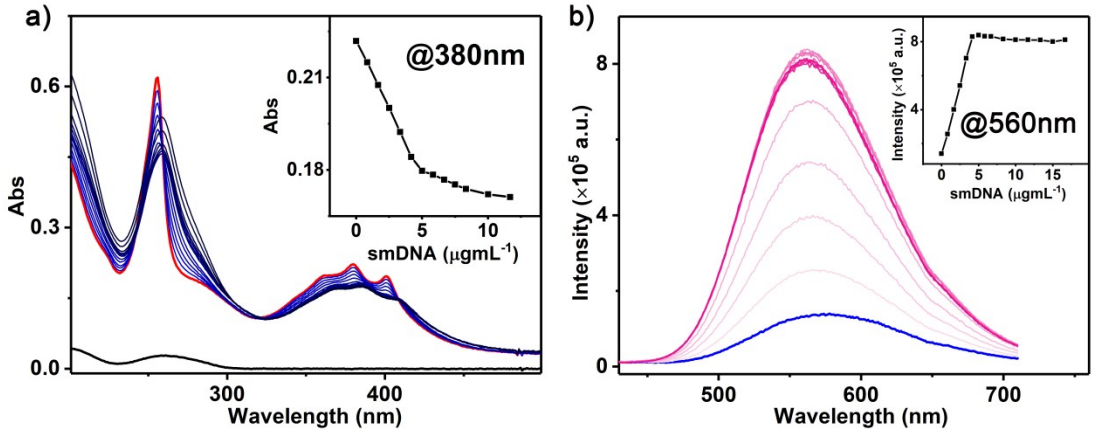

Figure S54. (a) UV-vis absorption and (b) fluorescence spectra of **2**•4Cl^{-} (10 μM) in water upon addition of smDNA. λ_{ex} = 365 nm, Ex/Em slit = 3 nm.

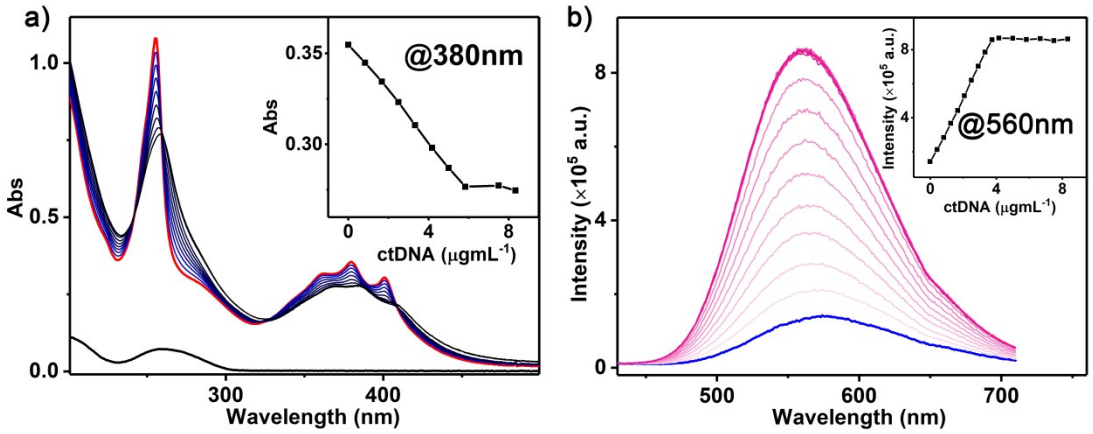

Figure S55. (a) UV-vis absorption and (b) fluorescence spectra of **2**•4Cl^{-} (10 μM) in water upon addition of ctDNA. λ_{ex} = 365 nm, Ex/Em slit = 3 nm.

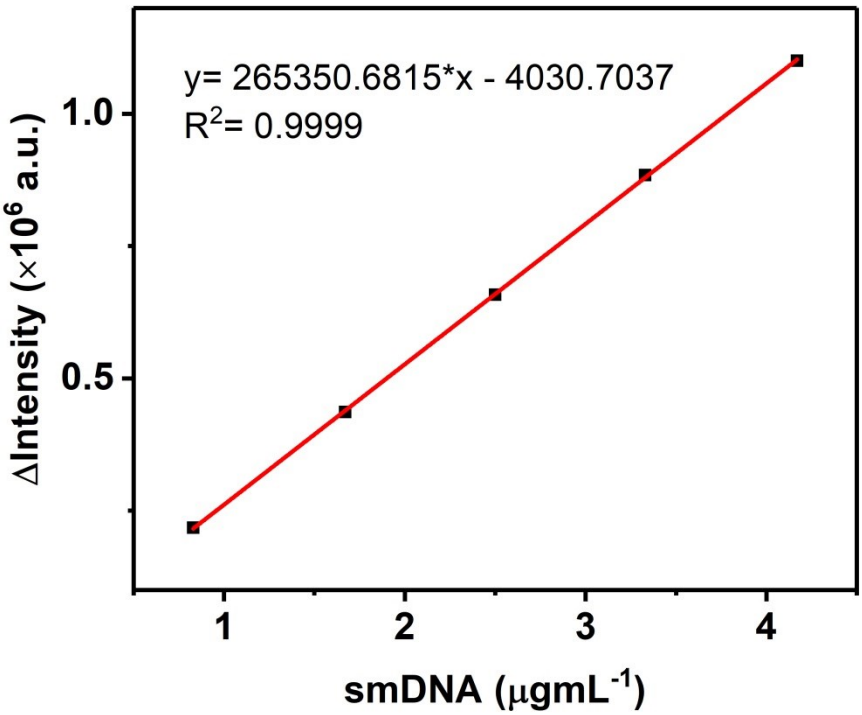

Figure S56. Change in fluorescence intensity of **1**•4Cl^{-} (10 μM) with smDNA concentration. y = 0, x = 0.0152 μgmL^{-1}.

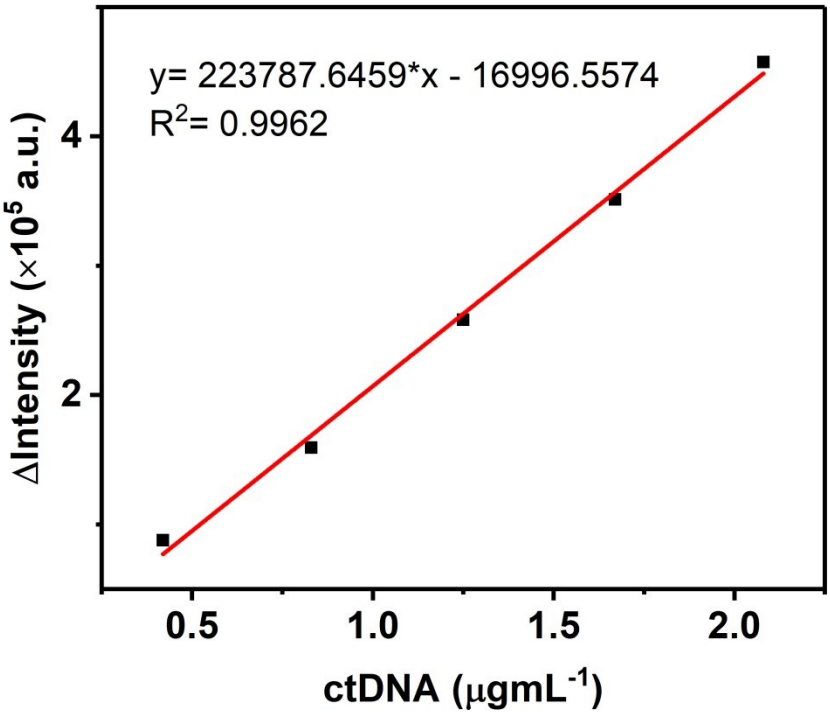

Figure S57. Change in fluorescence intensity of **1**•4Cl^{-} (10 μM) with ctDNA concentration. y = 0, x = 0.0759 μgmL^{-1}.

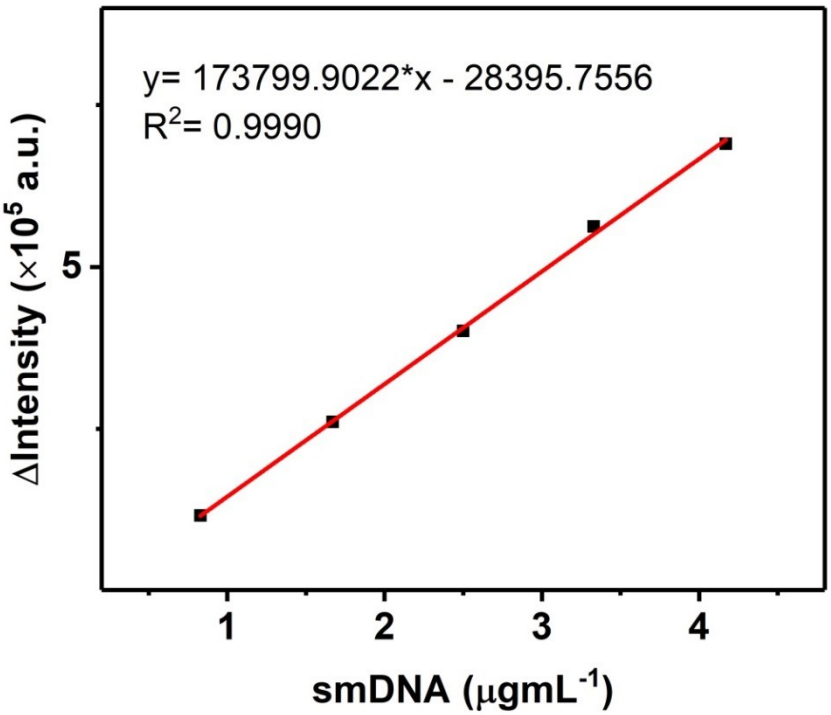

Figure S58. Change in fluorescence intensity of **2**•4Cl^{-} (10 μM) with smDNA concentration. y = 0, x = 0.1634 μgmL^{-1}. λ_{ex} = 365 nm, Ex/Em slit = 3 nm.

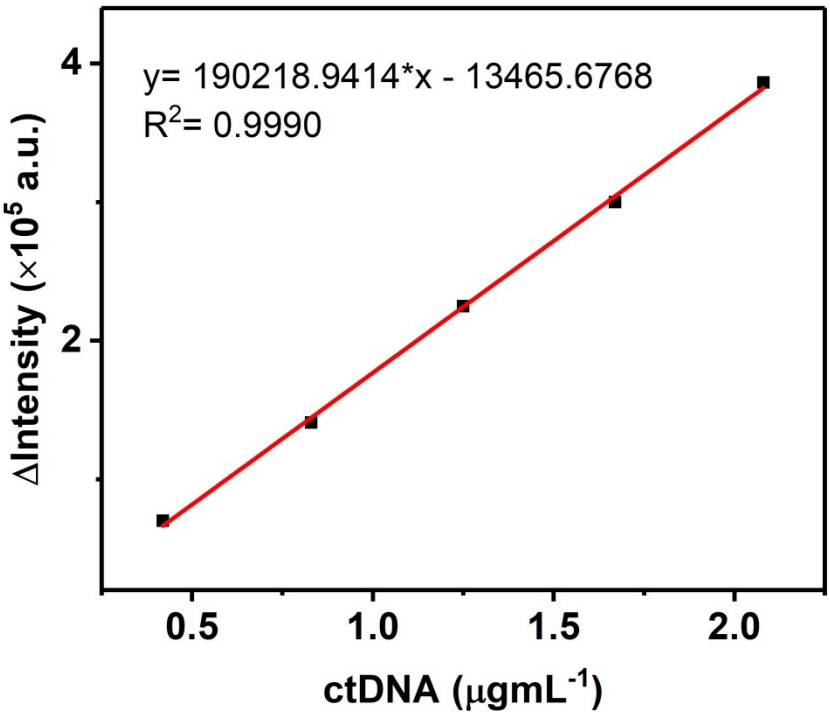

Figure S59. Change in fluorescence intensity of **2**•4Cl^{-} (10 μM) with ctDNA concentration. y = 0, x = 0.0708 μgmL^{-1}. λ_{ex} = 365 nm, Ex/Em slit = 3 nm.

CD titration and CPL experiment

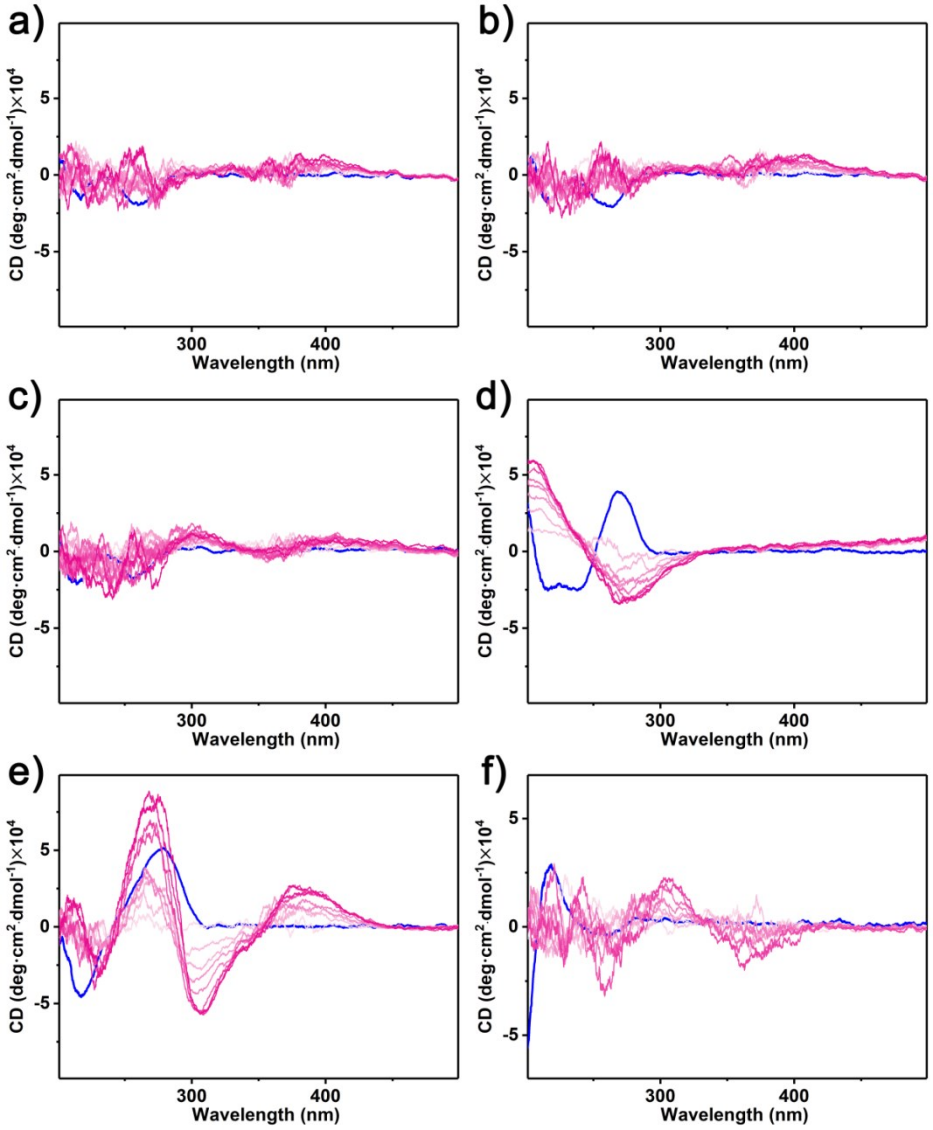

Figure S60. CD titration of **1**•4Cl^{-} (50 μM) with (a) AMP, (b) ADP, (c) ATP, (d) UTP, (e) CTP, (f) GTP in water.

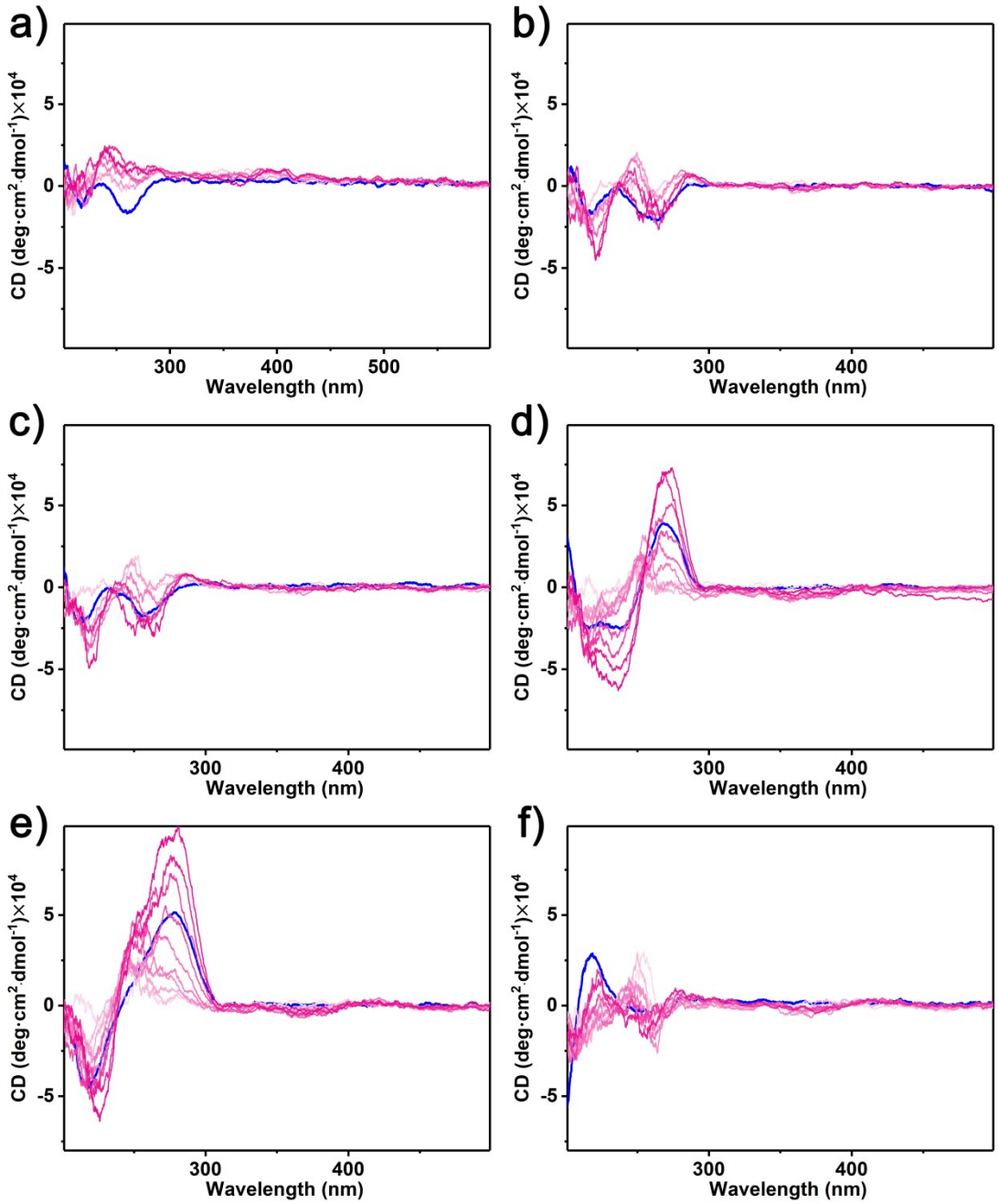

Figure S61. CD titration of **2**•4Cl¯ (50 μM) with (a) AMP, (b) ADP, (c) ATP, (d) UTP, (e) CTP, (f) GTP in water.

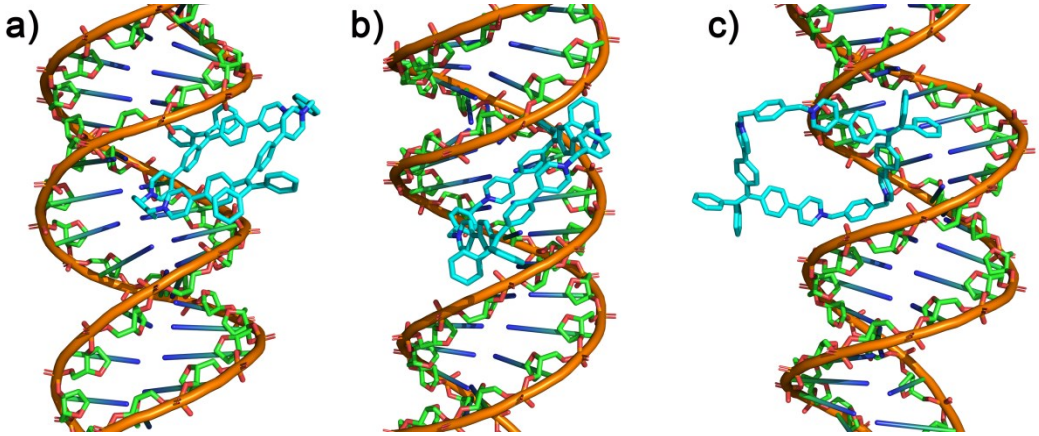

Figure S62. The molecular docking calculation of DNA□**1**.

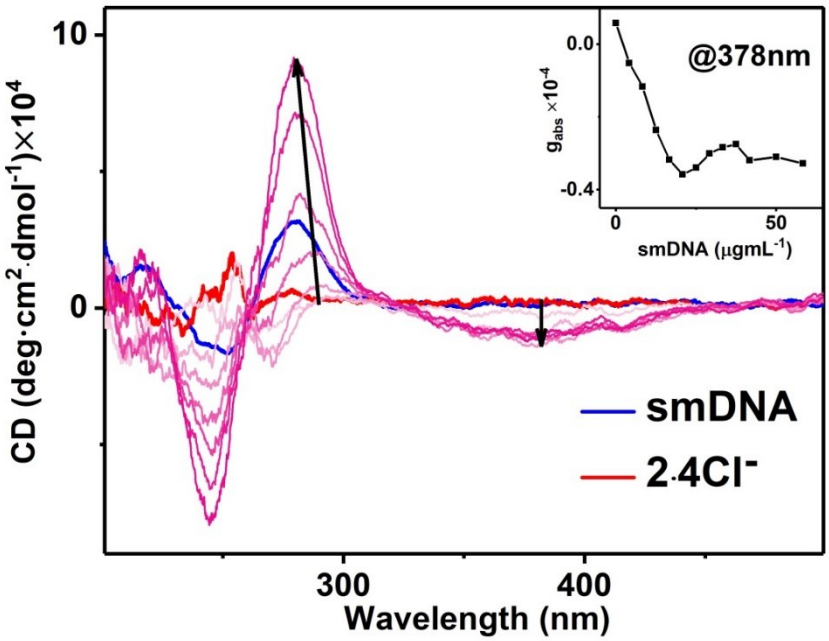

Figure S63. CD titration of **2**•4Cl¯ (50 μM) with smDNA in water. Insert: Plots of g_{abs} vs the equiv of guests.

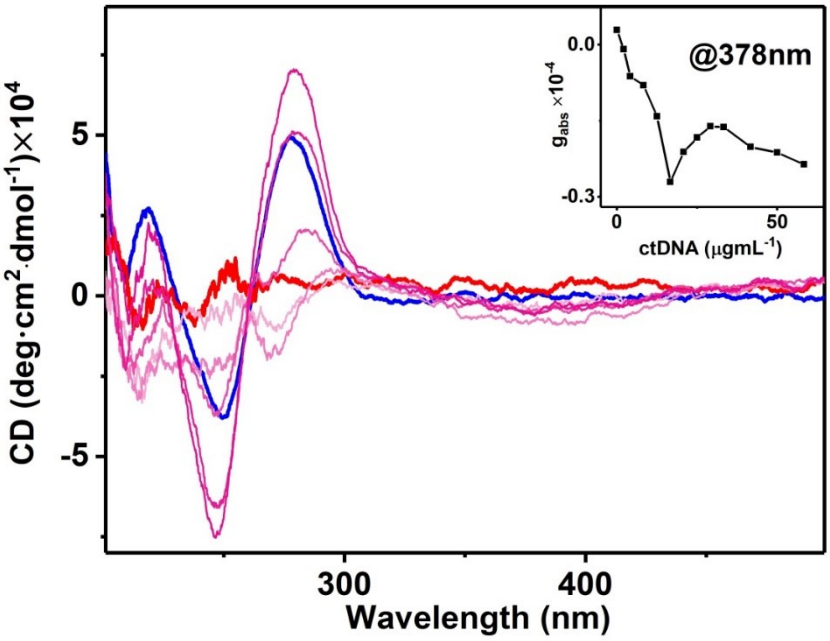

Figure S64. CD titration of **2**•4Cl$^-$ (50 μM) with ctDNA in water. Insert: Plots of g_{abs} vs the equiv of guests.

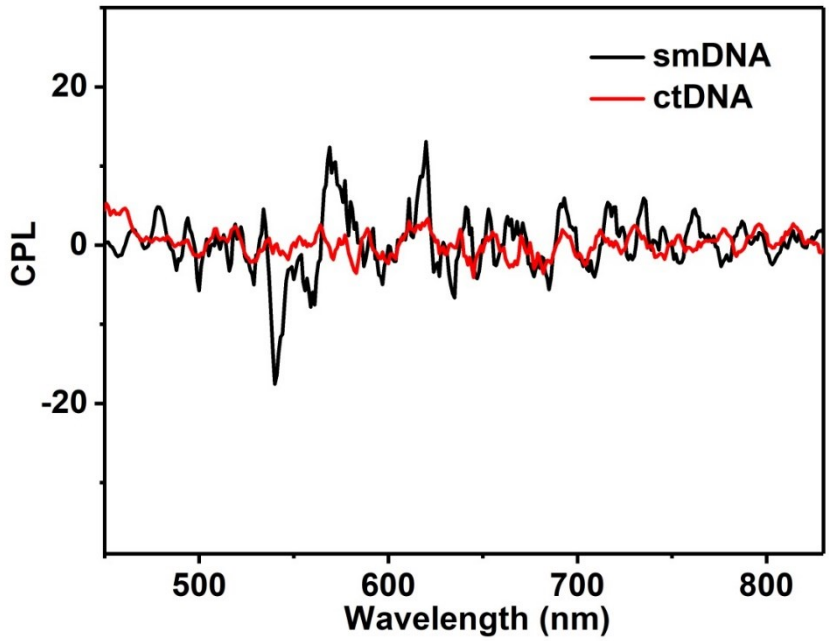

Figure S65. CPL of **1**•4Cl$^-$ (100 μM) with smDNA and ctDNA in water.

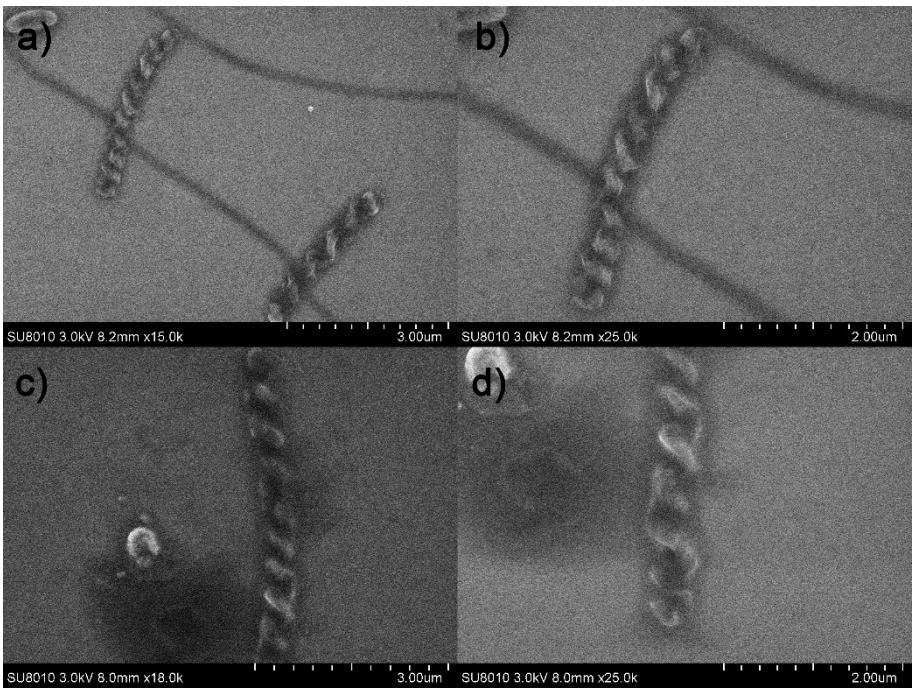

Figure S66. SEM images of (a)-(b) smDNA and (c)-(d) ctDNA in H_2O.

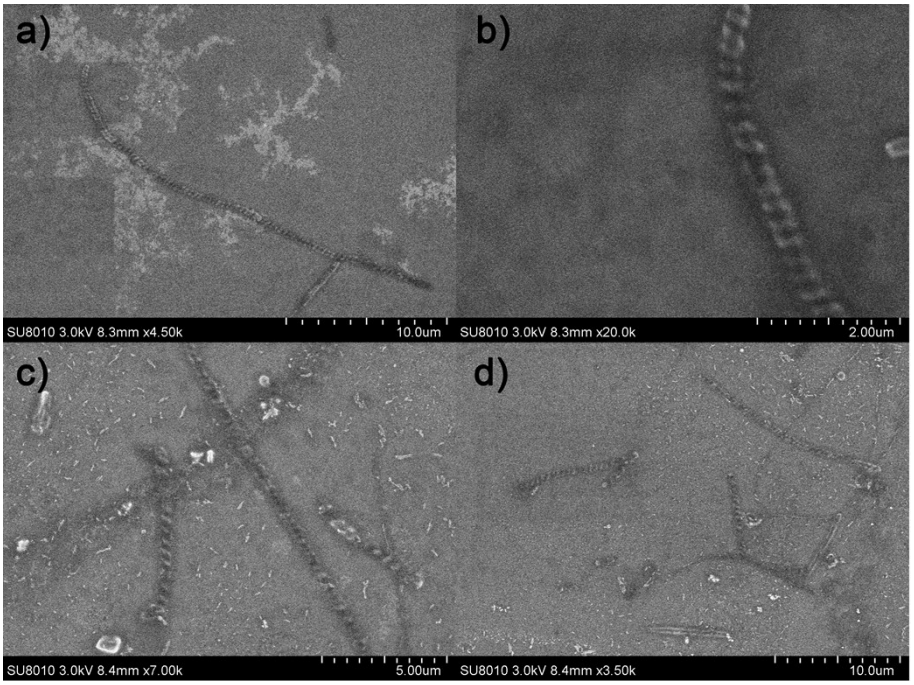

Figure S67. SEM images of (a)-(b) smDNA and (c)-(d) ctDNA with **1**•4Cl^- in H_2O.

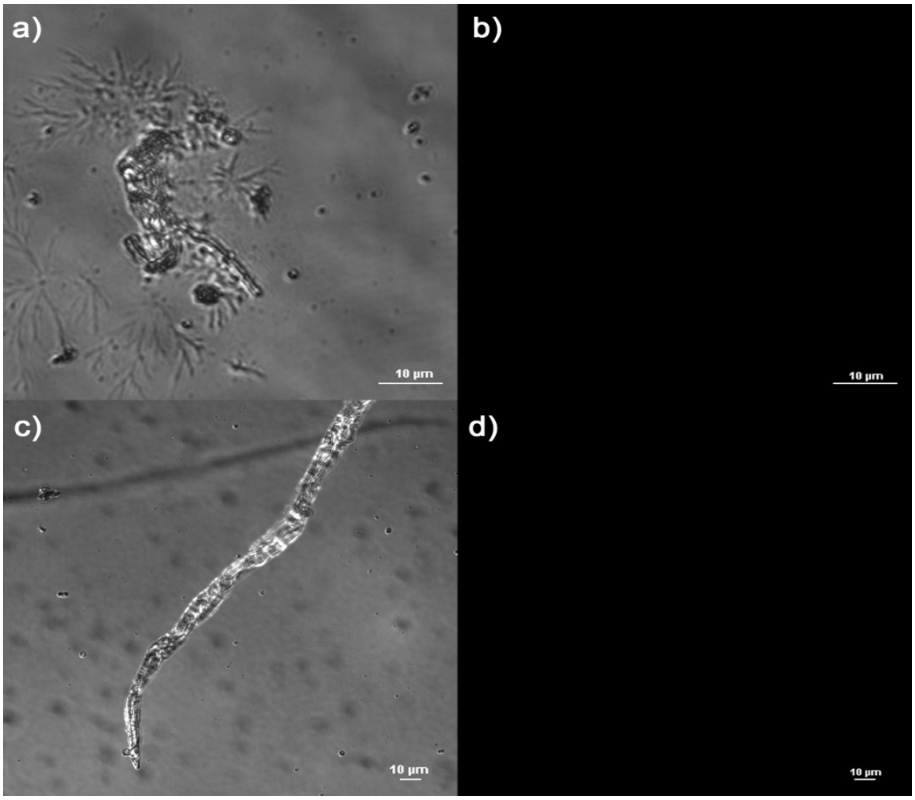

Figure S68. Confocal laser scanning microscope images of smDNA (a) bright-field images and (b) fluorescence images; ctDNA (c) bright-field images and (d) fluorescence images in H_2O. λ_{ex} = 405 nm.

Reference:

1. SAINT; part of Bruker APEX3 software package (version 2017.3.0): Bruker AXS, 2017.

2. SADABS; part of Bruker APEX3 software package (version 2017.3.0): Bruker AXS, 2017.

3. G. M. Sheldrick, *Acta Cryst.* **2015**, *A71*, 3-8.

4. G. M. Sheldrick, *Acta Cryst.* **2015**, *C71*, 3-8.

5. O.V. Dolomanov, L.J. Bourhis, R.J, Gildea, J.A.K. Howard, H. Puschmann, *J. Appl. Cryst.* **2009**, *42*, 339-341.

6. A. L. Spek, *Acta Cryst.* **2015**, *C71*, 9-19.